NJC

Accepted Manuscript

This article can be cited before page numbers have been issued, to do this please use: Á. Dancs, N. V. Nagy, K. Selmeczi, Z. Darula, A. Szorcsik, F. Matyuska, T. Páli and T. Gajda, *New J. Chem.*, 2016, DOI: 10.1039/C6NJ03126A.

This is an Accepted Manuscript, which has been through the Royal Society of Chemistry peer review process and has been accepted for publication.

Accepted Manuscripts are published online shortly after acceptance, before technical editing, formatting and proof reading. Using this free service, authors can make their results available to the community, in citable form, before we publish the edited article. We will replace this Accepted Manuscript with the edited and formatted Advance Article as soon as it is available.

You can find more information about Accepted Manuscripts in the author guidelines.

Please note that technical editing may introduce minor changes to the text and/or graphics, which may alter content. The journal's standard Terms & Conditions and the ethical guidelines, outlined in our author and reviewer resource centre, still apply. In no event shall the Royal Society of Chemistry be held responsible for any errors or omissions in this Accepted Manuscript or any consequences arising from the use of any information it contains.

View Article Online
DOI: 10.1039/C6NJ03126A

Tuning the coordination properties of multi-histidine peptides by using a tripodal scaffold: solution chemical study and catechol oxidase mimicking

Ágnes Dancs[a,c], Nóra May[b], Katalin Selmeczi[c], Zsuzsanna Darula[d], Attila Szorcsik[e], Ferenc Matyuska[a], Tibor Páli[f], Tamás Gajda[a,*]

[a] *Department of Inorganic and Analytical Chemistry, University of Szeged, Dóm tér 7, H-6720 Szeged, Hungary*
[b] *Institute of Organic Chemistry, Research Centre for Natural Sciences HAS, Magyar tudósok körútja 2, H-1117 Budapest, Hungary*
[c] *Université de Lorraine – CNRS, UMR 7565 SRSMC, BP 70239, 54506 Vandœuvre-lès-Nancy, France*
[d] *Institute of Biochemistry, Biologial Research Centre, Hungarian Academy of Sciences, Temesvári krt. 62, H-6724 Szeged, Hungary*
[e] *MTA-SZTE Bioinorganic Chemistry Research Group, Dóm tér 7, H-6720 Szeged, Hungary*
[f] *Institute of Biophysics, Biological Research Centre, Hungarian Academy of Sciences, Temesvári krt. 62, H-6724 Szeged, Hungary*

Abstract

Two new histidine-containing tripodal peptides containing non-protected N-terminal (**L**^{1}, tren3his) and C-terminal (**L**^{2}, nta3his) histidines have been synthesized in order to combine the structuring effect of tripodal scaffolds and the strong metal binding properties of histidine moieties. In the present work the copper(II) complexes of these ligands have been studied by combined pH-metric, UV-Vis, CD, EPR and MS methods. At 1:1 metal-to-ligand ratio the two ligands behave as the corresponding dipeptides containing N/C-terminal histidines, but above pH 9 the participation of the tertiary amine in the fused chelate rings results in unique binding modes in case of both ligands. Besides, the formation of oligonuclear complexes also confirms the positive influence of tripodal platforms on metal coordination, and provides the potential to be efficient functional models of oxidase enzymes. Accordingly, the oligonuclear complexes of both ligands have considerable catecholase-like activity. The oxidation of 3,5-di-*tert*-butyl-catechol proceeds with the participation of separated Cu^{2+} centers in presence of **L**^{1} complexes. However, the proximity of the two metal ions in the dinuclear complexes of **L**^{2} allows their cooperation along the catalytic cycle. Substrate binding modes, effect of reactants, intermediate and side product formation have also been studied, allowing to propose a plausible catalytic mechanism for each copper(II)-ligand systems.

**Corresponding author.*
E-mail: gajda@chem.u-szeged.hu (T. Gajda), Tel.: (+36)-62-544435, Fax: (+36)-62-544340

View Article Online
DOI: 10.1039/C6NJ03126A

1. Introduction

Linear peptides have long since been used to mimic the metal binding sites of metalloproteins[1-7] and metalloenzymes.[8-12] Previously, we also studied some histidine-rich peptides in order to create similar metal ion environment to native enzymes.[1,6,8-11] Such metallopeptides may possess notable catalytic activity to promote either hydrolytic[8,14] or redox[9-13] reactions. However, from structural point of view, linear peptides may only be useful to mimic metal binding sites of native enzymes, if the residues involved in the coordination are part of a relatively short sequence. Even is this case, the side-chain donors have relatively low metal binding ability in the physiological pH range as compared to the proteins, mainly due to the lack of pre-organized (tertiary) structure. As a consequence, amide coordinated complexes are formed in the presence of copper(II) at the neutral pH range.[9-12] In the case of multiple copper(II) binding, the metal ions are well separated along the peptide chain, eliminating the structural analogies to the native protein with oligonuclear active centers.

To avoid these difficulties, preorganized ligands with more favorable spatial distribution of the donor sites should be used. Recently, a cyclic His-rich decapeptide has been shown to be an efficient scaffold for highly stable multiimidazole coordination.[15] Tripodal peptidomimetics are also suitable for this purpose. Several tripodal peptides with different platforms have been designed as receptors of either organic molecules[16] or metal ions.[17-29] These ligands have several advantages in addition to the pre-organized structure and enhanced chelate effect. Using different amino acids, it is relatively easy to fine-tune the metal ion binding ability. Adequate substitution of the tripodal platform may influence the electronic structure and steric environment of the metal centers and may ensure the formation of oligonuclear complexes with relatively short metal-metal separation, which would allow the cooperation of metal centers during the catalytic processes.

Only a few reports are available in the literature describing metal ion interactions with tripodal peptides,[17-28] most of them are related to sulphur-containing ligands.[17-21] A series of nitrilotriacetic acid (nta) based tripodal cysteine or methionine derivatives were studied by Delangle *et al.* as selective chelators for copper(I).[16-20] These ligands have very high copper(I) binding ability, and form both mono- and oligonuclear complexes. Cysteine ethylester attached to benzene-1,3,5-tricarboxylic acid or tris(carboxyethyl)nitromethane as tripodal platforms were used to mimic Zn(II)-thiolate interaction in different metalloproteins, however, the formation of water-insoluble polymeric zinc(II) complexes was detected.[21] Two

View Article Online
DOI: 10.1039/C6NJ03126A

tricarboxylic acids have been used[22] as template to build up tripodal histidine-containing oligopeptides as models of carbonic anhydrase. Although their zinc(II) complexes have rather low solubility, the zinc(II)-bound water molecule in the $\{3N_{im},H_2O\}$ coordinated complexes have surprisingly low pK values (pK_a = 6.2). Zinc(II) complexes of *N*-benzyl-histidyl(ester)-substituted nta and tris-(2-aminoethyl)amine (tren) have been shown to efficiently mimic zinc(II) containing hydrolases.[23,24] Amino-protected histidines have also been linked to a triazacyclophane scaffold as a model of $\{3N_{im}\}$ coordinated copper(II) found in several metalloproteins.[25] A tren-based, alanine-containing tripodal ligand (tris[(L)-alanyl-2-carboxamidoethyl]amine) forms highly stable, amide coordinated mono- and dinuclear complexes with copper(II).[26] Copper(II) complexes of some histidine-containing branched peptides have also been studied.[27,28] Surprisingly, oligonuclear complexes were not detected in spite of the high number of available donor sites.

Our aim was to take advantage of the preorganized structure of tripodal scaffolds and the metal binding ability of histidine units in order to develop new oligometallic copper(II) cores, which may potentially mimic the function of oxidase enzymes. Although a number of reports has been published on the SOD mimicking properties of copper(II)-peptide complexes,[10-12] only a few can be found on their oxidase activity.[9,13,29-37] Several copper(II)-bound ATCUN-type peptides are able to oxidatively cleave DNA.[13,29] Copper(II) complexes of amyloid β 1-42 peptide (Aβ) promote oxidative damage to lipid membranes in presence of ascorbate,[30] while the dimeric adduct of Cu(II)-Aβ is able to oxidize cholesterol.[31] Copper(II) bound to different fragments of Aβ has been reported to have phenol and catechol oxidase-like activity, too.[32-34] However, such activity was questioned recently, and attributed to the presence of the chromophoric reagent 3-methyl-2-benzothiazolinone hydrazone.[35] Nevertheless, we[9] and others[36,37] also reported that copper(II) complexes of multihistidine peptides may possess (rather modest) cathecol oxidase mimicking properties.

Since the coordination chemistry of copper(II) complexes of non-protected histidines attached to tripodal platforms have not yet been explored, in this work we synthesized two new histidine derivatives based on tren and nta as tripodal platforms (Scheme 1), which contain N- and C-terminal histidines, respectively. Here we report solution equilibrium and spectroscopic study on the copper(II) binding properties. To screen the oxidase mimetic properties of these complexes, their catecholase activity was also studied by using 3,5-di-*tert*-butylcatechol (H_2DTBC) as model substrate.

View Article Online
DOI: 10.1039/C6NJ03126A

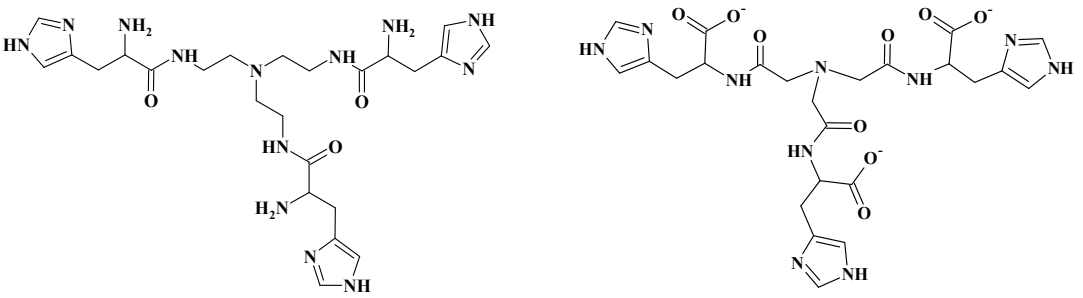

tren3his nta3his

Scheme 1 Schematic structure of the studied ligands.

2. Experimental Section

2.1. Materials

Copper(II) perchlorate (Sigma-Aldrich) stock solution was standardized complexometrically. pH-metric titrations were performed using 0.1 M NaOH standard solution (Sigma-Aldrich). *N*-α-*N*-im-di-Boc-L-histidine dicyclohexylammonium salt (Boc-His(Boc)-OH · DCHA, Aldrich), tris(2-aminoethyl)amine (tren, Sigma-Aldrich), L-histidine methylester dihydrochloride (Sigma-Aldrich), nitrilotriacetic acid (nta, Fluka), *N,N'*-dicyclohexylcarbodiimide (DCC, Sigma), *N*-hydroxybenzotriazole (HOBt, Novabiochem), 3,5-di-*tert*-butylcatechol (Fluka), 4-(2-hydroxyethyl)-1-piperazineethanesulfonic acid (HEPES, Sigma-Aldrich), *N*-cyclohexyl-2-aminoethanesulfonic acid (CHES, Sigma-Aldrich), 4-nitrocatechol (Sigma-Aldrich), dichloromethane (Molar Chemicals), chloroform (VWR) acetonitrile (VWR), ethyl acetate (VWR), trifluoroacetic acid (TFA, Sigma-Aldrich), triethylamine (Reanal) and triisopropylsilane (Sigma-Aldrich) were analytically pure chemicals and used without further purification.

2.2. Synthesis of tris[L-histidyl-2-carboxamidoethyl]amine (tren3his, L^1)

3 g Boc-His(Boc)-OH dicyclohexylammonium salt (5.59 mmol) was suspended in 100 ml ethyl acetate, washed with 30 ml ice cold phosphorous acid solution (10 (m/m)%) and cold water until neutral pH. The acidic phase was washed with 40 ml fresh cold ethyl acetate. The organic phases were combined, free Boc-His(Boc)-OH was obtained after evaporation of ethyl acetate solvent. 1.38 g Boc-His(Boc)-OH (3.88 mmol), 0.225 g tren (1.54 mmol), 0.55 g HOBt (4.07 mmol) and 0.83 g DCC (4.02 mmol) were dissolved in 40 ml dichloromethane with stirring. After 3 h at room temperature the white precipitate (dicyclohexylurea) was

View Article Online
DOI: 10.1039/C6NJ03126A

removed by filtration and dichloromethane was evaporated from the remaining solution. The residue was treated with a mixture of 95 (V/V)% TFA, 2.5 (V/V)% diisopropylsilane and 2.5 (V/V)% distilled water in order to remove N-protecting Boc-groups. TFA was evaporated, the oily product was dissolved in water, filtered and purified by preparative HPLC (reverse-phase column: Supelco C18 5 μm, 25 cm × 10 mm geometry, 0 to 4.1% acetonitrile+0.05% TFA/20 min. gradient elution mode, 3 ml/min flow rate, t_R' = 8.6 min). After liophilization we obtained the trifluoroacetate salt of **L^1** as white hygroscopic solid (61% yield). ^{1}H NMR (500 MHz, D_2O/H_2O, pH 7.19) δ (ppm): 2.46 (m, 6H, N_{tert}-CH_2), 2.98 (m, 6H, βCH_2), 3.18 (m, 6H, CH_2-NHCO), 3.88 (t, 3H, J = 7.0 Hz, αCH), 6.96 (s, 3H, im C^5H), 7.74 (s, 3H, im C^2H). ESI-MS **(**Finnigan TSQ-7000) *m/z* calcd for $C_{24}H_{40}N_{13}O_3$ $[M + H]^+$ 558.34, found 557.97 (z = 1) and $[M + 2H]^{2+}$ 278.98 (z = 2) (Fig. S1 in ESI).

2.3. Synthesis of tris-(L-histidyl)-2,2',2''-nitrilotriacetamide (nta3his, L^2)

1 g L-histidine methylester dihydrochloride (4.13 mmol) and 0.852 g DCC (4.13 mmol), 0.558 g HOBt (4.13 mmol) coupling agents were dissolved in 60 ml chloroform in presence of triethylamine (1.2 ml). A solution of nitrilotriacetic acid (0.26 g, 1.36 mmol) was added to the mixture and stirred at room temperature overnight. Chloroform was evaporated, the oily residue was treated with 5 eq. NaOH solution (H_2O:MeOH 2:1). The hydrolysis of methyl ester group was completed in 17 h at rt. Excess base was neutralized, the mixture was filtered and purified by preparative HPLC (column described above; conditions: 0 to 5% acetonitrile+0.1% TFA/20 min. gradient elution mode, 3 mlmin^{-1} flow rate, t_R' = 14.8 min). After purification and liophilization, **L^2** was obtained as a trifluoroacetate salt (yield 53%). ^{1}H NMR (500 MHz, D_2O/H_2O, pH 7.08) δ (ppm): 2.95 (dd, 3H, J_{AB} = 15.3 Hz, J_{HH} = 4.5 Hz, βCH_2), 2.96 (d, 3H, J_{AB} = 15.3 Hz, N_{tert}-CH_2), 3.06 (d, 3H, J_{AB} = 15.3 Hz, N_{tert}-CH_2), 3.16 (dd, 3H, J_{AB} = 15.3 Hz, J_{HH} = 4.5 Hz, βCH_2), 7.00 (s, 3H, im C^5H), 7.99 (s, 3H, im C^2H), 8.30 (d, 3H, CONH). ESI-MS **(**Finnigan TSQ-7000) *m/z* calcd for $C_{24}H_{31}N_{10}O_9$ $[M + H]^+$ 603.23, found 603.2 (z = 1) and $[M + 2H]^{2+}$ 302.0 (z = 2) (Fig. S2 in ESI).

2.4. Potentiometric measurements

The protonation and coordination equilibria were investigated by pH-potentiometric titrations in aqueous solutions (I = 0.1 M NaCl and T = 298.0 ± 0.1 K) under argon atmosphere. The titrations were performed using a PC controlled Dosimat 665 (Metrohm) automatic burette and an Orion 710A precision digital pH-meter. The Metrohm micro glass electrode (125 mm)

View Article Online
DOI: 10.1039/C6NJ03126A

was calibrated by the titration of hydrochloric acid and the data were fitted using the modified Nernst-equation[38]:

$$E = E_0 + K \cdot \log[\mathrm{H}^+] + J_{\mathrm{H}} \cdot [\mathrm{H}^+] + \frac{J_{\mathrm{OH}} \cdot K_{\mathrm{w}}}{[\mathrm{H}^+]}$$

where J_H and J_{OH} are the fitting parameters representing the acidic and alkaline error of the glass electrode, respectively ($K_w = 10^{-13.75}$ is the autoprotolysis constant of water[39]). The parameters were calculated by the non-linear least squares method. The formation of the complexes was characterized by the general equilibrium process:

$$\mathrm{pM} + \mathrm{qH} + \mathrm{rL} \rightleftharpoons \mathrm{M_pH_qL_r} \quad \beta_{\mathrm{M_pH_qL_r}}$$

$$\beta_{\mathrm{M_pH_qL_r}} = \frac{[\mathrm{M_pH_qL_r}]}{[\mathrm{M}]^{\mathrm{p}}[\mathrm{H}]^{\mathrm{q}}[\mathrm{L}]^{\mathrm{r}}}$$

where M denotes the metal ion and L the fully deprotonated ligand molecule. Charges are omitted for simplicity, but can be easily calculated taking into account the composition of the protonated ligand at pH 2 ($[H_6\mathbf{L^1}]^{6+}$ and $[H_6\mathbf{L^2}]^{3+}$). The protonation constants of the ligands and the formation constants of the complexes were calculated by the PSEQUAD computer program[40] from 4, and 6-8 independent titrations respectively (*ca*. 90 data points per titration). The metal ion concentrations varied between 1.5-3.3×10^{-3} M, using 2:1, 3:2, 1:1 and 1:2 metal-to-ligand ratios.

2.5. UV-visible absorption (UV-Vis) and circular dichroism (CD) spectroscopic measurements

The UV-Vis spectra were recorded on a Unicam Helios α spectrophotometer using a quartz cuvette with 1 cm optical pathlength. The CD spectra were measured on a Jasco J-710 spectropolarimeter in the wavelength interval from 300 to 900 nm in a cell with 1 cm optical pathlength. Spectral changes were monitored between pH 2 and 11 at 1:1 and 3:2 Cu(II)-$\mathbf{L^1}$, and 1:1 and 2:1 Cu(II)-$\mathbf{L^2}$ ratios. The metal ion concentration varied between 1.3-1.9×10^{-3} M and 1.5-2.9×10^{-3} M in the UV-Vis and 2.5-3.7×10^{-3} M and 1.5-2.9×10^{-3} M in the CD measurements for $\mathbf{L^1}$ and $\mathbf{L^2}$ titrations, respectively. The pH-dependent UV-Vis and CD spectra were processed together with the pH-potentiometric data using the PSEQUAD computer program,[40] resulting log β values as well as individual UV-Vis and CD spectra of the Cu(II) complexes. Kinetics and substrate binding measurements were performed on a Unicam Helios α and a PerkinElmer Lambda 1050 spectrophotometer.

View Article Online
DOI: 10.1039/C6NJ03126A

2.6. EPR measurements

EPR spectra of the copper(II) complexes were recorded on a BRUKER EleXsys E500 spectrometer (microwave frequency 9.81 GHz, microwave power 10 mW, modulation amplitude 5 G, modulation frequency 100 kHz) at room temperature. The pH-dependent series of EPR spectra of Cu(II)-**L**^{1} complexes (pH = 2.3 – 11.3) were collected under argon atmosphere, in both equimolar solution ($0.95\times c_L = c_{Cu^{2+}} = 1.6\times10^{-3}$ M) and at metal ion excess ($1.40\times c_L = c_{Cu^{2+}} = 2.31\times10^{-3}$ M) in a circulating system using a Heidolph Pumpdrive 5101 peristaltic pump. The ionic strength was adjusted to 0.1 M with NaCl. The pH of the solution was measured using a Radiometer PHM240 pH/ion Meter equipped with a Metrohm 6.0234.100 glass electrode. The two series of room-temperature CW-EPR spectra were simulated by the 2D_EPR program.[41] This program simulates all the recorded isotropic spectra by fitting the EPR parameters of all the paramagnetic species and their formation constants simultaneously. For copper(II) complexes the parameters g_o, A_o^{Cu} copper hyperfine (I_{Cu}= 3/2) and A_o^{N} nitrogen (I_N = 1) hyperfine coupling has been taken into account to describe each component curve. The relaxation parameters, α, β, and γ defined the linewidths through the equation $\sigma_{MI}=\alpha+\beta M_I+\gamma M_I^2$, where M_I denotes the magnetic quantum number of copper(II) ion. Since common copper(II) perchlorate was used for the measurements, the spectra were calculated by the summation of spectra ^{63}Cu and ^{65}Cu weighted by their natural abundances. The hyperfine and the relaxation parameters were obtained in field units (Gauss = 10^{-4} T).

EPR spectra of Cu(II)-**L**^{2} system have been measured using individually prepared and pH-adjusted solutions (I = 0.1 M NaCl), at 1:1 and 2:1 metal-to-ligand ratios ($c_{Cu^{2+}} = 1.7\times10^{-3}$-$3.3\times10^{-3}$ M). The isotropic EPR spectra were recorded at room temperature in a glass capillary. Samples of 100 µl were placed in a quartz EPR tube and measured in a dewar containing liquid nitrogen (77 K) to obtain anisotropic EPR spectra (25 µl methanol was added to each sample to avoid water crystallization). Isotropic EPR spectra were fitted by the "EPR" program[42] using the parameters: g_o, A_o^{Cu} copper hyperfine (I_{Cu}= 3/2) and A_o^{N} nitrogen (I_N = 1) hyperfine couplings, as detailed above. The anisotropic EPR spectra recorded at 77 K were also analyzed by the "EPR" program. For the *g*- and *A*- tensor rhombic symmetry have been found and fitted by the main values of g_x, g_y and g_z, and copper hyperfine parameters A_x^{Cu}, A_y^{Cu} and A_z^{Cu}. In case when well resolved superhyperfine lines were detected, a rhombic

View Article Online
DOI: 10.1039/C6NJ03126A

nitrogen coupling were taken into account (a_x^N, a_y^N, a_z^N) as well. The linewidths have been described by the above equation using orientation dependent α, β and γ parameters.

Detection of the oxygenated radical intermediate was carried out using a Bruker ECS106 X-band EPR spectrometer (modulation amplitude 0.84 G, microwave power 5 mW, 5×10^4 receiver gain, 16 scans). After mixing the reaction solution under aerobic conditions (in EtOH/H_2O 50/50 HEPES/CHES buffer, I = 0.1 M, $c_{complex} = 5\times10^{-5}$ M, $c_{H_2DTBC} = 2\times10^{-3}$ M, pH = 8), a sample of 4-5 µl was put in a capillary tube, and measured in presence of 2,2-diphenyl-1-picrylhydrazyl (DPPH) internal reference.

2.7. Matrix-assisted-laser desorption/ionization time-of-flight mass spectrometric (MALDI-TOF MS) measurements

Molecular weight analysis of the formed complexes was executed by MALDI-TOF MS, using a BRUKER REFLEX III MALDI-TOF mass spectrometer. The samples were prepared in aqueous solutions at ligand-to-metal ratios 3:2 (**L**^{1}) and 2:1 (**L**^{2}) by adjusting the desired pH using NaOH and HCl solutions. 1 µl of the samples was spotted onto the MALDI target plate and let dry before adding 0.5 µl of the matrix solution (20 mg/ml 2,5-dihydroxybenzoic acid (DHB) in water or 2,6-dihydroxyacetophenone (DHAP) in ACN:water 1:1). Mass spectra were recorded in the positive (**L**^{1} complexes) and negative (**L**^{2} complexes) reflectron mode collecting 200 shots for each sample (*m/z* range: 900-2000). External calibration affording ±200 ppm mass accuracy was performed using peptide standards. DHB and DHAP matrices were obtained from Sigma-Aldrich.

2.8. Oxidation of 3,5-di-tert-butylcatechol

Kinetic study. The oxidation of 3,5-di-*tert*-butylcatechol (H_2DTBC) was followed in buffered solutions (0.02 M HEPES/CHES, I = 0.1 M (0.08 M NaCl), T = 298 K) by detecting the increase in absorption at 400 nm of 3,5-di-*tert*-butyl-*o*-benzoquinone (DTBQ, ε = 1900 $M^{-1}cm^{-1}$). 50% ethanol-50% aqueous solutions were used to prevent the precipitation of DTBQ. The actual pH in this mixed solvent was determined by adding 0.21 units to the pH-meter reading,[43] the auto-ionization constant of water in this medium is pK_w = 14.84.[44] O_2 excess was obtained by addition of EtOH saturated by O_2 gas to the reaction solutions (the solubility of O_2 is 250 $mgdm^{-3}$ and 41 $mgdm^{-3}$ in ethanol and water, respectively[45]). After mixing the ethanol and the aqueous phases, the solutions were thermostated at 298 K for 2-3 minutes, then the reaction was initiated by the addition of H_2DTBC as ethanolic solution.

View Article Online
DOI: 10.1039/C6NJ03126A

According to the initial reaction rates (v_i) method, the experimental data used for the calculations corresponded to ~ 4% conversion of the initial substrate concentration. k_{obs} values were determined under pseudo-first order conditions, from the slope of the increasing absorbance according to the following equation:

$$v_i = d[DTBQ]/dt = (\varepsilon_{400nm} \times l)^{-1} \times (dA/dt) = k_{obs} \times [S]_o$$

where dA/dt is the slope of the fitted curve, ε_{400} is the molar absorptivity of DTBQ at 400 nm, l is the optical pathlength, and $[S]_o$ is the initial concentration of the substrate.

Autooxidation of H_2DTBC was taken into account in every experiments, resulting $k_{obs,corr}$ values ($k_{obs,corr} = k_{obs} - k_{obs,auto}$). The parameters of the Michaelis-Menten model (K_M and k_{cat}) were calculated by non-linear least square method. The reported kinetic data are averages of at least three parallel measurements. Note that for kinetic measurements, $c_{complex}$ corresponds to the concentration of all trinuclear ($\mathbf{L^1}$) or dinuclear ($\mathbf{L^2}$) complexes at the given pH, regardless of their current protonation states. Experimental turnover values have been determined by following reactions for 1 h in open cuvette cells, allowing oxygen supplement from air.

Substrate binding study. Substrate binding experiments were carried out in buffered 50% ethanol-water solutions (0.05 M HEPES/CHES, I = 0.1 M (0.05 M NaCl), T = 298 K). During the study of 4-nitrocatechol ($H_2$4NC) binding the complex concentrations varied between 0.8 - 2.5×10^{-4} M or was held constant on 2.1×10^{-5} M. Deprotonation constants and spectroscopic parameters of 4NC species were calculated using PSEQUAD program.[40]

Anaerobic H_2DTBC binding UV-Vis measurements were executed under argon atmosphere, in closed quartz cuvette equipped with a septum, with 1 cm optical pathlength. Different volumes of H_2DTBC stock solution were added to the closed cuvette containing the buffered complex solutions (both deoxygenated) using a Hamilton syringe, and after equilibration the spectra were recorded. Complex concentrations were 2.4×10^{-4} M in case of each ligand system, substrate concentration varied between 0-1.2×10^{-2} M. 'Blank' experiments, in the absence of metal complexes, were also carried out to verify the anaerobic conditions. Every experiments were repeated (2 parallels) in order to confirm reproducibility.

Detection of H_2O_2. The formation of hydrogen peroxide during the oxidation of H_2DTBC was identified and quantified spectrophotometrically, as $[Ti(O_2)(OH)]^+$ complex ($\lambda^{408\ nm}$ = 935 $M^{-1}cm^{-1}$), in aqueous solutions, in presence of Cu(II)-$\mathbf{L^1}$ 3:2 (pH = 7.8) or Cu(II)-$\mathbf{L^2}$ 2:1 (pH = 8.5) complexes. In a typical experiment, 20 ml oxygenated reaction solution has been prepared (0.02 M HEPES/CHES, I = 0.1 M (0.08 M NaCl), T = 298 K) and the reaction was started by adding the appropriate amount of H_2DTBC. After different time intervals (t = 1, 6,

View Article Online
DOI: 10.1039/C6NJ03126A

12 and 30 min) 4.5 ml aliquots have been removed and extracted with 2×5 ml dichloromethane, in order to eliminate the residual substrate and benzoquinone product. The aqueous phases were treated with excess H_2SO_4 and $TiOSO_4$ solutions, and subsequently measured in a quartz cuvette of 1 cm pathlength. Complex concentrations were 5×10^{-5} M, the initial H_2DTBC concentration was 2×10^{-3} M. The production of DTBQ has been also determined under identical conditions, but without the extraction step. After a given time interval 1:1 HCl solution was added to stop the reaction, and to dissolve the DTBQ formed during the reaction, the solution was mixed with ethanol to obtain 50 % ethanol-water mixture.

3. Results and Discussion

In the present work the copper(II) complexes of two new histidine-containing tripodal peptides containing non-protected N-terminal ($\mathbf{L^1}$, tren3his) and C-terminal ($\mathbf{L^2}$, nta3his) histidines have been studied. The ligands have been synthesized by solution phase peptide synthesis, followed by the purification using preparative HPLC.

3.1. Protonation of the ligands

For both $\mathbf{L^1}$ and $\mathbf{L^2}$ six pK values could be determined between pH 2-11 (listed in Table 1 headline). Although the protonation processes of $\mathbf{L^1}$ are strongly overlapped, the first three pK values are mostly related to deprotonation of the imidazole rings, while pK_4, pK_5 and pK_6 to those of the amino groups. The deprotonation processes of $\mathbf{L^2}$ are more separated. In the acidic region the carboxylic, above pH 6 the imidazolium groups deprotonate. The average imidazole pK values of the two ligands ($pK_{im,\mathbf{L^1}} = 4.63$, $pK_{im,\mathbf{L^2}} = 7.11$) show notable basicity difference. This indicates that the imidazolium/imidazole rings are involved in strong H-bonding network with the positively charged ammonium groups ($\mathbf{L^1}$) and negatively charged carboxylates ($\mathbf{L^2}$). In addition, the high overall charge of $\mathbf{L^1}$ in the acidic pH (*e.g.* $(H_6\mathbf{L^1})^{6+}$) also increases the acidity of imidazolium rings.

Protonation of the tertiary amines were not detected in the studied pH range,[46] these are deprotonated at pH 2 in case of both ligands (p$K \leq 1.5$).

View Article Online
DOI: 10.1039/C6NJ03126A

Table 1 Formation constants and spectroscopic (UV-Vis, CD and EPR) parameters of copper(II)-$\mathbf{L^1}$ complexes (estimated errors in parentheses (last digit), I = 0.1 M NaCl, T = 298 K). The protonation constants ($\log\beta_{0q1}$) values of $\mathbf{L^1}$ from q = 1 ($[H\mathbf{L^1}]^{+}$) to q = 6 ($[H_6\mathbf{L^1}]^{6+}$) are: 7.85(1), 15.06(1), 21.40(1), 26.60(1), 31.42(1), 35.29(1).

$Cu_pH_qL_r$	$\log\beta_{pqr}$ [a]	$\lambda^{d\text{-}d}_{max}$ (nm), ε ($M^{-1}cm^{-1}$)	λ^{CD}_{max} (nm), $\Delta\varepsilon$ ($M^{-1}cm^{-1}$)	g_o	A_o (G)
131	29.32(1)[a] [29.21(3)][b]	650, 56.3	630, 0.41 312, -0.42	2.136(2)	61(1)
121	25.66(1)[a] [25.54(4)][b]	602, 99.9	624, 0.96 318, -0.93	2.109(6)	71.3(7)
111	20.11(1)[a] [19.95(9)][b]	614, 107.7	654, 0.76 318, -0.77	2.112(6)	68.7(6)
101	13.19(1)[a] [13.18(9)][b]	638, 100.5	690, 0.65 318, -0.55	2.111(6)	59.5(6)
1-11	4.07(2)[a] [4.01(6)][b]	626, 155.0	715, 0.64 612, -0.15	2.106(3)	9(5)
1-21	-6.80(2)[a] [-6.84(5)][b]	596, 200.8	708, -0.62 582, 0.60 312, 1.64	2.089(3)	63(3)
322	49.57(2)[a] [49.60(4)][b]	626, 189.0	636, 1.82 318, -1.82	2.102(3)[c] 2.133(2)[c]	64.1(7)[c] 48.7(6)[c]
302	38.20(3)[a,d]	630, 198.2	678, 1.57 318, -1.30	2.103(2)	57(3)
3-12	30.93(4)[a,d]	638. 264.7	702, 1.46 546, 0.30 312, -1.09	2.124(3)	60(2)
3-22	22.73(4)[a,d]	632, 262.2	708, 1.92 594, -0.49	2.106(4)	61(3)
3-32	14.03(4)[a,d]	616, 304.3	714, 1.57 612, -0.05 312, 0.42	2.099(2)	51(4)
3-42	3.77(4)[a,d]	614, 329.5	690, -0.88 576, 1.57 318, 5.20	2.107(3)	52(3)
3-52	-6.99(3)[a,d]	610, 320.5	702, -0.38 582, 1.57 318, 4.40	2.097(3)	56(2)

[a]$\log\beta$ values derived from the combined potentiometric and CD spectroscopic data
[b]$\log\beta$ values derived from the pH-dependent EPR data
[c]EPR parameters of $Cu_3H_2L_2$ component spectra; see text in details
[d]during the evaluation of EPR spectra, the formation constants of these species were taken from the potentiometric data, due to the their weakly resolved and nearly identical spectra.

View Article Online
DOI: 10.1039/C6NJ03126A

3.2. Copper(II) complexes of tren3his

The speciation in the copper(II)-$\mathbf{L}^{\mathbf{1}}$ system proved to be rather complicated. Therefore, beside the combined evaluation of potentiometric and CD data, pH-dependent EPR titration was also used to uncover the equilibrium properties. The two independent sets of formation constants, derived from our potentiometric/CD and EPR titrations, are in good agreement (Table 1).

These formation constants are related to a given composition, which in turn may exist in forms of structural isomers. Based on the spectroscopic information discussed later, we were able to identify the main isomers, but due to the polidentate nature of the ligand others with smaller mole fraction may also exist.

In equimolar solution, four differently protonated mononuclear complexes are formed up to pH 8 (Fig. 1A).

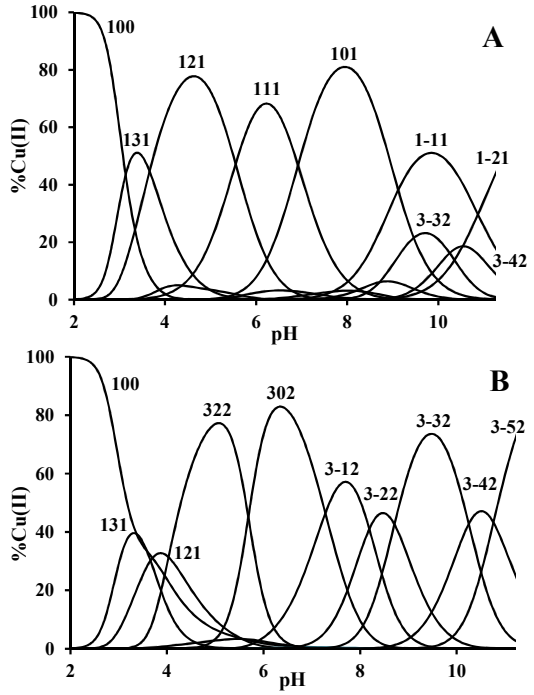

Figure 1 Speciation diagrams of Cu(II)-$\mathbf{L}^{\mathbf{1}}$ 1:1 (**A**) and 3:2 (**B**) system ($c_{\mathbf{L}^{\mathbf{1}}} = c_{Cu(II)} = 0.001$ M and $1.5 \times c_{\mathbf{L}^{\mathbf{1}}} = c_{Cu(II)} = 0.001$ M respectively, $I = 0.1$ M NaCl, $T = 298$ K).

Both the spectroscopic data ($\lambda^{d\text{-}d}_{max} = 644$ nm, weak positive CD peak at ~ 640 nm, $g_o = 2.124$, $A_o = 53$ G) and the equilibrium constant of the reaction $Cu^{2+} + H_3\mathbf{L}^{\mathbf{1}} = CuH_3\mathbf{L}^{\mathbf{1}}$ ($\log K = \log\beta_{131} - \log\beta_{031} = 7.92$) are consistent with a $\{3N_{im}\}$ coordination in $CuH_3\mathbf{L}^{\mathbf{1}}$.[9,47] In case of peptides with N-terminal histidine, the *bis*-histamine-like $\{2NH_2,2N_{im}\}$ coordination is preferred in the neutral pH range.[48,49] In principle, this binding mode may appear already in

View Article Online
DOI: 10.1039/C6NJ03126A

$CuH_2\mathbf{L}^1$. However, during the successive deprotonations $CuH_3\mathbf{L}^1 \rightarrow CuH_2\mathbf{L}^1 \rightarrow CuH\mathbf{L}^1 \rightarrow Cu\mathbf{L}^1$ the visible**,** CD and EPR spectra all show significant changes (Figs. S3, 2A, 3A).

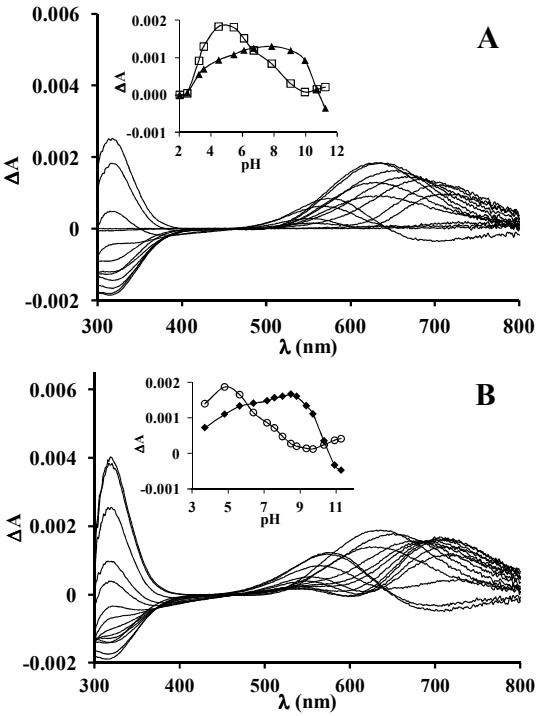

Figure 2 pH-dependent CD spectra of Cu(II)-$\mathbf{L}^1$ 1:1 (**A**) and 3:2 (**B**) system ($c_{\mathbf{L}^1} = c_{Cu(II)}$ = 0.0025 M and $1.5 \times c_{\mathbf{L}^1} = c_{Cu(II)}$ = 0.0037 M respectively, I = 0.1 M NaCl, T = 298 K). Insert: pH-dependence of Δε at 630 nm (□ and ○) and 700 nm (▲ and ♦).

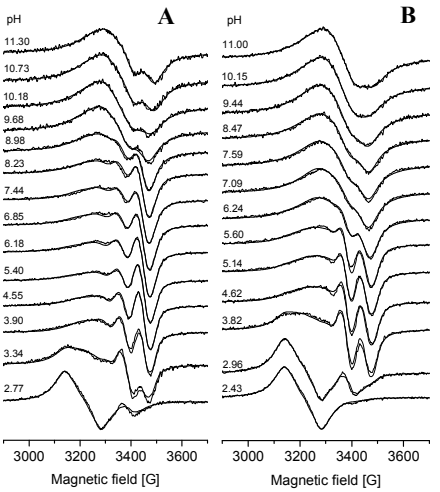

View Article Online
DOI: 10.1039/C6NJ03126A

Figure 3 pH-dependent EPR spectra of Cu(II)-$\mathbf{L^1}$ 1:1 (**A**) and 3:2 (**B**) system ($0.95\times c_{\mathbf{L1}} = c_{Cu(II)} = 0.0016$ M and $1.4\times c_{\mathbf{L1}} = c_{Cu(II)} = 0.0023$ M respectively, $I = 0.1$ M NaCl, $T = 298$ K).

Moreover, the pK values of the above-mentioned successive deprotonations ($pK_{CuH_3\mathbf{L1}} = 3.71$, $pK_{CuH_2\mathbf{L1}} = 5.55$, $pK_{CuH\mathbf{L1}} = 6.92$) are considerably smaller than the corresponding values of the free ligand ($pK_{H_3\mathbf{L1}} = 6.34$, $pK_{H_2\mathbf{L1}} = 7.25$, $pK_{H\mathbf{L1}} = 7.85$), indicating copper(II) promoted deprotonations. All these facts suggest continuous changes in the coordination environment of the metal ion during the processes $CuH_3\mathbf{L^1} \rightarrow CuH_2\mathbf{L^1} \rightarrow CuH\mathbf{L^1} \rightarrow Cu\mathbf{L^1}$. The spectroscopic parameters of $CuH_2\mathbf{L^1}$ ($\lambda^{d\text{-}d}_{max} = 602$ nm, $g_o = 2.109$, $A_o = 71.3$ G) indicate considerably increased ligand field strength as compared to $CuH_3\mathbf{L^1}$, which supports the coordination of four nitrogens in $CuH_2\mathbf{L^1}$, thus $\{NH_2,3N_{im}\}$ binding mode in the equatorial plane of copper(II). The copper(II) promoted deprotonation of the second amino nitrogen of $\mathbf{L^1}$ should lead to the highly stable *bis*-histamine-like $\{2NH_2,2N_{im}\}$ coordination in the equatorial plane of $CuH\mathbf{L^1}$. However, the slight red shift of the d-d transitions and the decrease of A_o of this species ($\lambda^{d\text{-}d}_{max} = 615$ nm, $g_o = 2.112$, $A_o = 68.7$ G) as compared to $CuH_2\mathbf{L^1}$, indicate some distortion of the crystal field around the metal ion. Considering that five N-donors are available for metal ion binding in $CuH\mathbf{L^1}$, this distortion is most likely caused by the axial coordination of the third imidazole nitrogen $\{2NH_2,2N_{im}+N_{im}\}$. During the next copper(II) promoted deprotonation ($CuH\mathbf{L^1} \rightarrow Cu\mathbf{L^1}$) an even more important red shift of the visible/CD spectra and decrease of A_o was observed ($\lambda^{d\text{-}d}_{max} = 640$ nm, $g_o = 2.111$, $A_o = 59.5$ G). Since the 6N coordinated *tris*-histamine-like complex of copper(II) is not known even in the case of histamine,[50] the observed spectral changes are due to the replacement of the axially coordinated imidazole ring by the third amino group in $Cu\mathbf{L^1}$ ($\{2NH_2,2N_{im} + NH_2\}$, see Scheme 2).

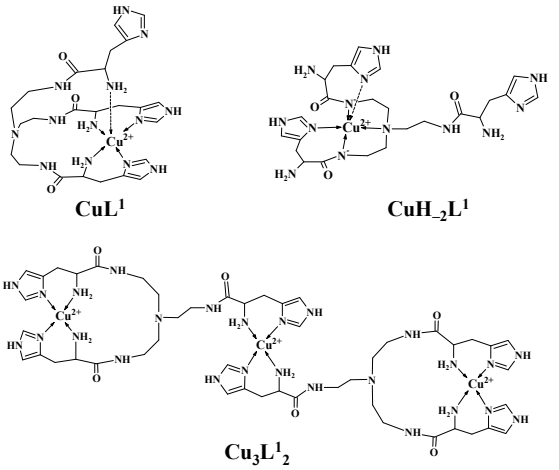

View Article Online
DOI: 10.1039/C6NJ03126A

Scheme 2 Proposed schematic structure of some copper(II)-$\mathbf{L^1}$ complexes (dashed arrow line indicates possible axial coordination).

At higher pH, further deprotonations were observed leading to the species $CuH_{-1}\mathbf{L^1}$ and $CuH_{-2}\mathbf{L^1}$. Due to the notable stability of $Cu\mathbf{L^1}$ (log$K$ = 13.19), these deprotonations take place only above pH 8 (p$K_{Cu\mathbf{L^1}}$ = 9.12 and p$K_{CuH_{-1}\mathbf{L^1}}$ = 10.87), at higher pH than usual for peptides with N-terminal His moieties.[28,51,52] Such processes can be related to the metal ion promoted deprotonation of amide nitrogen(s), water molecule(s), or in certain cases coordinated imidazole ring(s).[1] The increasing negative contribution in the visible CD spectra of $CuH_{-1}\mathbf{L^1}$ and $CuH_{-2}\mathbf{L^1}$ indicates metal ion induced deprotonation and coordination of amide nitrogen(s) in our system,[53] according to the high affinity of copper(II) toward amide nitrogens. The rather unique visible CD spectrum (as well as the visible and EPR spectra) determined for the species $CuH_{-2}\mathbf{L^1}$ is nearly identical to those of the $CuH_{-2}L$ complexes of Ac-HGG-NH_2, Ac-HGGG-NH_2, Ac-HGGGW-NH_2 and several other analogues of prion protein octarepeat domain.[54-56] Based on this similarity, in $CuH_{-2}\mathbf{L^1}$ we suggest $\{N_{im},N^-,N_{tert},N^-\}$ coordination (Scheme 2) in the equatorial plane of the metal ion (for a more detailed discussion of the possible structures of $CuH_{-1}\mathbf{L^1}$ and $CuH_{-2}\mathbf{L^1}$, see the Electronic Supplementary Information).

The presence of at least ten potential nitrogen donors in $\mathbf{L^1}$ may provide the possibility to the formation of oligonuclear complexes, too. Indeed, at 3:2 metal-to-ligand ratio the solution was clear in the whole studied pH range, but precipitate was observed above pH 6 at 2:1 metal-to-ligand ratio. This observation indicates the formation of trinuclear complexes with $Cu_3H_x\mathbf{L^1}_2$ stoichiometry. The presence of such species, beside the mononuclear complexes, was confirmed by MALDI-TOF MS at pH ~ 10. The isotopic distribution patterns obtained (Fig. 4) are in very good agreement with those calculated for the molecular ions $[CuH_{-1}\mathbf{L^1}]^+$ (=$[CuC_{24}H_{38}O_3N_{13}]^+$) and $[Cu_3H_{-5}\mathbf{L^1}_2]^+$ (=$[Cu_3C_{48}H_{73}O_6N_{26}]^+$). There are differences, however, between the estimated and measured molecular weights (619.24/620.36 and 1298.41/1301.32), which corresponds to the uptake of one and three protons, respectively. The measured higher molecular weights is due to the reduction of Cu^{2+} to Cu^+ and the corresponding uptake of one proton per metal ions during the ionization processes. Identical observations were reported in the literature related to MALDI-TOF MS studies of many copper(II) complexes, formed with cyclen/cyclam derivatives,[57] some pseudo-peptides[58] and peptides.[59]

View Article Online
DOI: 10.1039/C6NJ03126A

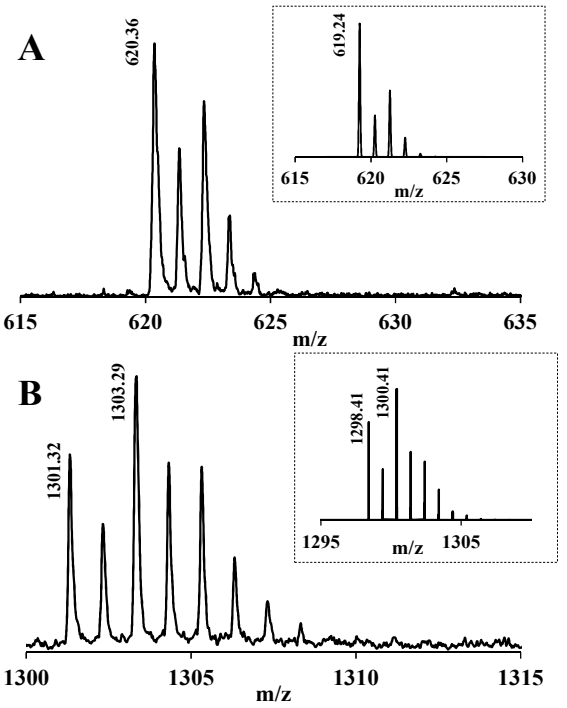

Figure 4 MALDI-TOF MS spectra measured in the Cu(II)-$\mathbf{L^1}$ 1:1 (**A**) and 3:2 (**B**) systems. Insert: calculated spectra of the corresponding complex ($[C_{24}H_{38}N_{13}O_3Cu]^+$ and $[C_{48}H_{73}N_{26}O_6Cu_3]^+$, respectively).

Since trinuclear complexes may have several protonation states, the copper(II)-$\mathbf{L^1}$ 3:2 system presents a complicated, but rather obvious speciation behavior (Fig. 1B). $Cu_3H_2\mathbf{L^1}_2$ is the first trinuclear complex formed around pH 5. Considering the ten available N-donors (the additional two are still protonated), the three copper(II) ions have 3/4N coordination environments, similarly to those in the mononuclear complexes $CuH_3\mathbf{L^1}$ and $CuH_2\mathbf{L^1}$. Indeed, the evaluation of the pH-dependent EPR spectra indicated that the spectrum of $Cu_3H_2\mathbf{L^1}_2$ is the superposition of two, rather distinct component spectra having similar g_0 values to $CuH_3\mathbf{L^1}$ and $CuH_2\mathbf{L^1}$ (Table 1). All trinuclear complexes have detectable EPR spectra (Fig. 3B), indicating weakly interacting metal ions. Nevertheless, only the spectra of $Cu_3H_2\mathbf{L^1}_2$ and $Cu_3\mathbf{L^1}_2$ show comparatively well-resolved hyperfine structures. In $Cu_3\mathbf{L^1}_2$ the six N-terminal His units create *bis*-histamine-like coordination environment around the three metal ions. This is similar to that observed in $Cu\mathbf{L^1}$, except the axially coordinated amino group present in the latter. Accordingly, the UV-Vis (and CD) spectrum of $Cu_3\mathbf{L^1}_2$ shows ~ 20 nm blue shift as compared to that of $Cu\mathbf{L^1}$ (Table 1). Although other alternatives are also possible, the most likely structure of $Cu_3\mathbf{L^1}_2$ is depicted in Scheme 2. In principle, the three legs of $\mathbf{L^1}$ may induce the formation of higher oligomers with the composition $(Cu_3\mathbf{L^1}_2)_n$ (n > 1), too.

View Article Online
DOI: 10.1039/C6NJ03126A

However, the linewidth of the isotropic EPR spectra, especially at lower magnetic fields, is sensitive to the radius of the complex molecules. Since intensity loss was not observed, and the linewidth of the EPR spectrum of $Cu_3\mathbf{L^1}_2$ is similar to that of the analogous $Cu_2(dhen)_2$ complex,[51] the formation of higher oligomers is at least negligible.

Above pH 6, consecutive deprotonations of the trinuclear complexes were observed (Fig. 1B). The characteristic CD spectra of $CuH_{-1}\mathbf{L^1}$ and $CuH_{-2}\mathbf{L^1}$ are very similar to those of $Cu_3H_{-2}\mathbf{L^1}_2$ and $Cu_3H_{-4}\mathbf{L^1}_2$, respectively (Fig. S4). Accordingly, in latter species two copper(II) ions have similar $\{N_{im},N^-,N_{tert},N^-\}$ coordination environment to the corresponding mononuclear complexes (Scheme 2). This in turn means that similar deprotonation processes take place at more than one log unit lower pH in the trinuclear complexes as compared to the mononuclear ones. This is probably due to the stabilization by the axial nitrogen coordination, which is present only in the mononuclear $Cu\mathbf{L^1}$ and $CuH_{-1}\mathbf{L^1}$ complexes. The fifth deprotonation ($Cu_3H_{-4}\mathbf{L^1}_2 = Cu_3H_{-5}\mathbf{L^1}_2 + H^+$, p$K$ = 10.76) does not result in considerable change of spectral properties. The central metal ion in the trinuclear complexes, bound to both ligands (Scheme S1), has clearly different coordination environment from the other two, since the histamine-like chelate rings belong to two different molecules, and thus fused chelates can not be formed between them. This coordination mode is identical to that in $Cu(His\text{-}Gly)_2$ complex, which also undergoes a single deprotonation at high pH.[48,60]

3.3. Copper(II) complexes of nta3his

The presence of three C-terminal histidines in $\mathbf{L^2}$ also provides the possibility of the formation of oligonuclear complexes. Indeed, the comparative evaluation of the experimental data indicated the formation of 6 mononuclear and 4 dinuclear complexes (Table 2, Fig. 5).

Table 2 Formation constants and characteristic spectroscopic (UV-Vis and CD) parameters of copper(II)-$\mathbf{L^2}$ complexes (estimated errors in parentheses (last digit), I = 0.1 M NaCl, T = 298 K). The protonation constants ($\log\beta_{0q1}$) values of $\mathbf{L^2}$ from q = 1 ($[H\mathbf{L^2}]^{2-}$) to q = 6 ($[H_6\mathbf{L^2}]^{3+}$) are: 7.83(1), 14.87(1), 21.33(1), 24.64(1), 27.07(1), 29.36(1).

$Cu_pH_qL_r$	$\log\beta_{pqr}$	$\lambda^{d\text{-}d}_{max}$ (nm), ε ($M^{-1}cm^{-1}$)	λ^{CD}_{max} (nm), $\Delta\varepsilon$ ($M^{-1}cm^{-1}$)
131	25.64(1)	640, 71.6	305, -0.64 545, 0.27 635, -0.17
121	22.50(2)	625, 91.6	305, -1.19 545, 0.59 630, -0.31

View Article Online
DOI: 10.1039/C6NJ03126A

111	18.97(2)	625, 88.5	310, -0.89 545, 0.73 635, -0.22
101	12.77(3)	625, 90.3	310, -0.85 550, 0.74 635, -0.20
1-11	5.40(3)	627, 91.9	310, -0.69 550, 0.66 640, -0.18
1-21	-5.21(4)	650, 109.5	630, -1.53 780, 0.82
201	17.84(1)	650, 118.4	310, -0.80 550, 0.66
2-11	12.56(1)	665, 142.3	315, -0.61 560, 0.90 705, 0.47
2-21	5.91(1)	605, 179.5	305, -3.09 525, 1.01 665, -0.59
2-31	-3.42(1)	630, 180.8	310, -2.34 570, 1.01 650, 0.96

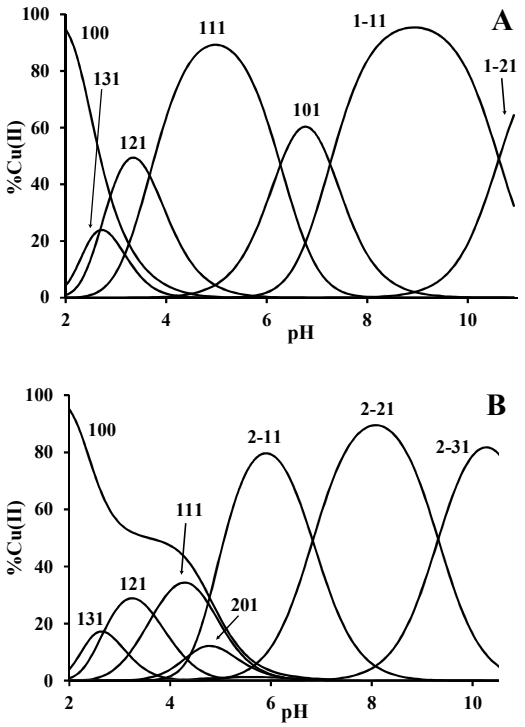

Figure 5 Speciation diagrams of Cu(II)-$\mathbf{L^2}$ 1:1 (**A**) and 2:1 (**B**) system ($c_{\mathbf{L^2}} = c_{Cu(II)} = 0.001$ M and $2\times c_{\mathbf{L^2}} = c_{Cu(II)} = 0.002$ M respectively, $I = 0.1$ M NaCl, $T = 298$ K).

View Article Online
DOI: 10.1039/C6NJ03126A

Nevertheless, the speciation and the spectral properties of the complexes are much less complicated than in case of Cu(II)-$\mathbf{L^1}$ system. In equimolar solution, the visible and CD spectra are practically unchanged between pH 4 – 10 (Figs. 6A, S5A), and consequently the calculated individual visible and CD spectra of the species $CuH\mathbf{L^2}$, $Cu\mathbf{L^2}$, $CuH_{-1}\mathbf{L^2}$ are identical, and even those of $CuH_2\mathbf{L^2}$ are very similar (Figs. S6A, S7A). Moreover, the EPR spectra recorded at pH 4.9 and 8.9 are also identical (Fig. 7). It means that the coordination environment of copper(II) in these complexes is also identical, and the successive deprotonations are related to non-coordinating side chains. Indeed, the pK values of these deprotonations (pK = 3.14, 3.54, 6.20, 7.34, Table 2) are consistent with the proton loss of two carboxylic and two imidazole groups of the free ligand.

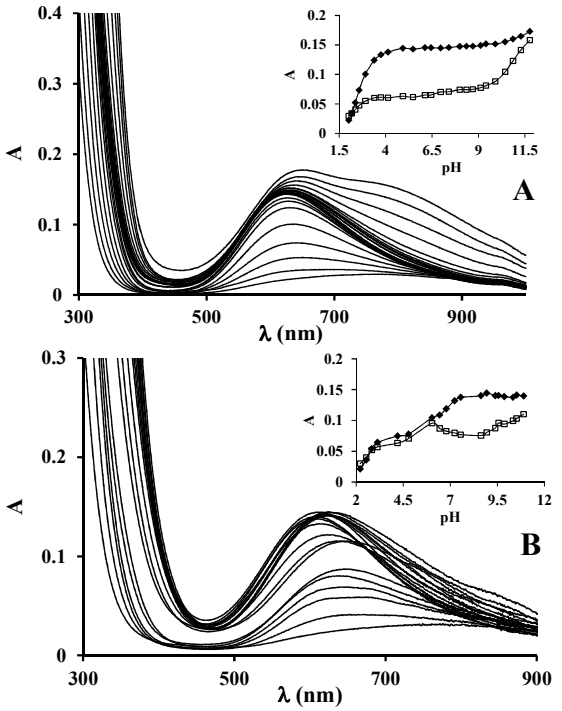

Figure 6 pH-dependent UV-Vis spectra of Cu(II)-$\mathbf{L^2}$ 1:1 (**A**) and 2:1 (**B**) system ($c_{\mathbf{L}^2} = c_{Cu(II)}$ = 0.0015 M and $1.95 \times c_{\mathbf{L}^2} = c_{Cu(II)}$ = 0.0029 M respectively, I = 0.1 M NaCl, T = 298 K). Insert: pH-dependent absorbances at 628 (♦) and 770 nm (□) for 1:1, 607 (♦) and 720 nm (□) for 2:1 Cu(II)-to-$\mathbf{L^2}$ ratio.

View Article Online
DOI: 10.1039/C6NJ03126A

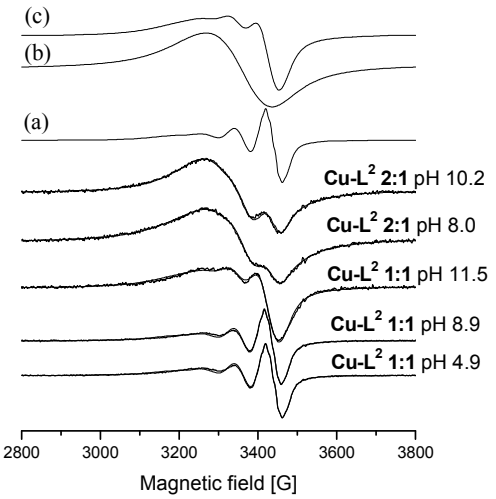

Figure 7 Isotropic EPR spectra recorded at 298 K in Cu(II)-$\mathbf{L^2}$ 1:1 and 2:1 systems ($c_{\mathbf{L^2}}$ = $c_{Cu(II)}$ = 0.0017 M and 1.9×$c_{\mathbf{L^2}}$ = $c_{Cu(II)}$ = 0.0033 M respectively, I = 0.1 M NaCl). Calculated EPR parameters of (a), (b) and (c) component spectra (related to the complexes $CuH_x\mathbf{L^2}$ (x = 2, 1, 0, -1), $Cu_2H_x\mathbf{L^2}$ (x = -1, -2, -3) and $CuH_{-2}\mathbf{L^2}$, respectively) are listed in Table S1.

The extra deprotonation detected for $CuH_{-1}\mathbf{L^2}$ and its intense CD spectra indicate the presence of a coordinated amide nitrogen in this, and therefore in all mentioned complexes. The spectroscopic parameters of $CuH_{-1}\mathbf{L^2}$ ($\lambda^{d\text{-}d}_{max}$ = 615 nm, g_o = 2.1121, A_o = 71.5 G, $g_{x/y/z}$ = 2.0448/2.0526/2.2285, $A_{x/y/z}$ = 17.4/8.6/178.9 G) are consistent with a $\{N_{tert},N^-,N_{im},O\}$ type coordination with slight rombic distortion, similarly to the $CuH_{-1}L$ complexes of Gly-His[60,61] or glycyl-histamine.[62] The high stability of the Gly-His-like coordination[48,49] explains the unchanged binding mode during four successive deprotonations of non-coordinated side-chains. The formation of the Gly-His-like $\{N_{tert},N^-,N_{im},O\}$ coordination mode in the present system takes place at somewhat lower pH than in the case of Gly-His itself,[52,60,61] which can be explained by the important basicity difference of the tertiary ($\mathbf{L^2}$) and primary (Gly-His) amines involved in the metal ion binding. In the copper(II)-Gly-His and related systems the fourth equatorial position is occupied by a water molecule, which deprotonates with a pK = 9.2 – 9.4.[48,60-62] In our system such deprotonation was not observed, indicating that the fourth equatorial position in $CuH_{-1}L$ is more likely occupied by an amide oxygen in chelating position (Scheme 3).

View Article Online
DOI: 10.1039/C6NJ03126A

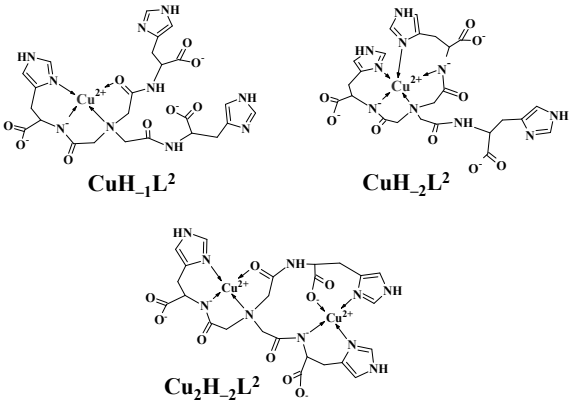

Scheme 3 Proposed schematic structure of some copper(II)-$\mathbf{L^2}$ complexes.

The formation of $CuH_{-2}\mathbf{L^2}$ above pH 10 results in fundamental changes of the spectroscopic behaviors. On the individual visible spectrum of this species two bands appear with nearly equal intensities at 645 and 765 nm (Fig. S6A), which may suggest an intermediate structure between square pyramidal and trigonal bipyramidal geometries,[63] which is rare in the case of copper(II)-peptide complexes. The intensity of the CD bands increases considerably in the d–d region (Figs. S5A, S7A), indicating the metal coordination of a further amide nitrogen, since only this binding can induce strong chiral perturbation. In general, the amide coordination results in an increase of the EPR parameter A_0, due to the increased ligand field around the metal ion. However, in the present case, A_0 of $CuH_{-2}\mathbf{L^2}$ (g_o = 2.1117, A_o = 61.8 G) is considerably smaller than that of the former species, indicating an axially coordinated nitrogen. Considering all these facts and the available unbound imidazole rings, an $\{N_{tert},2N^-,N_{im}+N_{im}\}$ type coordination is the most probable in $CuH_{-2}\mathbf{L^2}$ (Scheme 3). The alternative binding mode without the tertiary amine (*i.e.* $\{2N^-,2N_{im}\}$), which is rather common in the case of peptides containing the –HXH– sequence, has distinctly different spectral properties.[9,64]

The two non-coordinating C-terminal histidine legs in $CuH_x\mathbf{L^2}$ (x = 2, 1, 0, -1) obviously may bind further metal ion(s). Since the solution is clear in the whole studied pH range at 2:1 metal-to-ligand ratio, and further increasing metal ion excess resulted in precipitation around pH 6, only dinuclear complexes can be expected. Indeed, our experimental data indicate the formation of four dinuclear complexes above pH 4 (Fig. 5B). The presence of dicopper(II) complexes with 2:1 metal-to-ligand ratio was also confirmed by MALDI-TOF MS. The isotopic distribution pattern obtained is in agreement with that calculated for the molecular ion $[Cu\mathbf{L^2}]^- = [C_{24}H_{27}N_{10}O_9Cu]^-$ and $[Cu_2H_{-2}\mathbf{L^2}]^- = [C_{24}H_{25}N_{10}O_9Cu_2]^-$ (Fig. S9). However,

View Article Online
DOI: 10.1039/C6NJ03126A

there is a difference between the estimated (662.13, 723.04) and measured (663.26, 725.21) molecular weights. The difference is one mass unit per metal ion as before for copper(II)-$\mathbf{L^1}$ system, which is the result of the reduction of Cu^{2+} to Cu^{+} and the corresponding uptake of a proton during the ionization processes, as it was earlier observed for many copper(II) complexes.[57-59]

Considering the high stability of the above mentioned Gly-His-like $\{N_{tert},N^{-},N_{im},O\}$ coordination, one copper(II) should retain this binding mode in the dinuclear $Cu_2H_{-1}\mathbf{L^2}$ species. Indeed, the equilibrium constant for the process $CuH_{-1}\mathbf{L^2} + Cu^{2+} = Cu_2H_{-1}\mathbf{L^2}$ ($\log K$ = 7.2), as well as the visible and CD difference spectra between $Cu_2H_{-1}\mathbf{L^2}$ and $CuH_{-1}\mathbf{L^2}$ ($\lambda^{d\text{-}d}_{max}$ ~ 700 nm, positive CD band around 640 nm, Figs. S6B, S7B) are in accordance with a $\{2N_{im},2COO^{-}\}$ type coordination of the second metal ion in $Cu_2H_{-1}\mathbf{L^2}$.[65] The following deprotonation ($pK(Cu_2H_{-1}\mathbf{L^2})$ = 6.65) results in ~ 60 nm blue shift of the d-d maximum and important change on the CD spectra, which indicate amide nitrogen coordination to the second metal ion (the Gly-His-like coordination in the mononuclear complexes is unchanged up to pH 9). Indeed, the visible difference spectra between $Cu_2H_{-2}\mathbf{L^2}$ and $CuH_{-1}\mathbf{L^2}$ ($\lambda^{d\text{-}d}_{max}$ ~ 585 nm, Fig. S6B) is again in good accordance[65] with a $\{2N_{im},N^{-},COO^{-}\}$ type coordination (Scheme 3) in the equatorial plane of the second copper(II). This species has surprisingly high stability: it is the dominant complex over nearly 3 pH units. The next deprotonation ($pK(Cu_2H_{-2}\mathbf{L^2})$ = 9.35) induces further characteristic changes on CD spectra both in the UV and visible region (Figs. S5B, S7B), which reflects the metal coordination of the third amide nitrogen. On the other hand, the visible spectrum shows ~ 20 nm red shift between pH 8-10.3 (Fig. S6B). The spectral changes exclude the formation of a binding mode present in $CuH_{-2}\mathbf{L^2}$. The third amide nitrogen binds most likely to the second metal ion, creating a $\{N_{tert},N^{-},N_{im},O;\ 2N^{-},2N_{im}\}$ coordination mode in $Cu_2H_{-3}\mathbf{L^2}$. Peptides with -HXH- sequence undergo two strongly overlapping amide deprotonations, due to the preferred formation of a $\{2N^{-},2N_{im}\}$ coordinated species.[9,64] However, in the present case the two successive amide deprotonations are well separated, because they are involved in a considerably less favored eight-membered chelate ring. Moreover, this chelate ring contains the metal-bound tertiary amine, too, which probably makes the conformational change needed for the $Cu_2H_{-2}\mathbf{L^2} = Cu_2H_{-3}\mathbf{L^2} + H^{+}$ deprotonation more difficult, resulting in the dominant formation of $Cu_2H_{-2}\mathbf{L^2}$ at pH 8.

View Article Online
DOI: 10.1039/C6NJ03126A

3.4 Comparing the copper(II) binding properties of L^1 and L^2

At 1:1 metal-to-ligand ratio and between pH 5-9 the two ligands behave as the corresponding dipeptides containing N/C-terminal histidine. The multiimidazole environment present below pH 5 in $CuH_3\mathbf{L^1}$/$CuH_2\mathbf{L^1}$ switches to *bis*-histamine-like coordination in $CuH\mathbf{L^1}$/$Cu\mathbf{L^1}$, while at higher pH the participation of the tertiary amine in the fused chelate rings results in a unique $\{N_{im},N^-,N_{tert},N^-\}$ binding mode in $CuH_{-2}\mathbf{L^1}$. It means that above pH 5 only one free (loosely bound) N-terminal histidine leg is available for binding a further metal ion, which results in the formation of oligonuclear complexes with 3:2 metal-to-ligand ratio. Since the metal ion environment in the corresponding mono- and trinuclear complexes (*e.g.* in $Cu\mathbf{L^1}$ and $Cu_3\mathbf{L^1}_2$) are nearly identical, trinuclear complexes are present even at 1/1 metal-to-ligand ratio. On the other hand, the Gly-His-like coordination in $CuH_x\mathbf{L^2}$ (x = 2, 1, 0, -1) leaves two unbound C-terminal histidine legs, which provides the possibility for the formation of dinuclear species with 2:1 metal-to-ligand ratio. Consequently, the two metal binding sites of $\mathbf{L^2}$ are distinctly different, and due to the outstanding stability of Gly-His-like coordination dinuclear complexes are formed only at metal ion excess.

3.5. Oxidation of 3,5-di-tert-butylcatechol: kinetic study

Our intention was to develop a new oligometallic copper(II) core, which may potentially mimic the function of oxidase enzymes. Catechol oxidases are type 3 copper enzymes,[66,67] therefore mostly dinuclear complexes were used for the biomimetic studies.[68-74] Nevertheless, several mononuclear[75-77] or trinuclear[78] complexes were also reported to possess important catecholase-like activity. To screen the enzyme mimetic properties of our oligonuclear copper(II) complexes, their catecholase activity was investigated by using the widely studied 3,5-di-*tert*-butylcatechol (H_2DTBC) as model substrate. The formation of the oxidized product, 3,5-di-*tert*-butyl-*o*-benzoquinone (DTBQ) was followed spectrophotometrically at 400 nm. 50% EtOH/H_2O solvent was applied in order to prevent the precipitation of DTBQ.

Our preliminary data indicated that only the oligonuclear complexes possess notable catecholase-like properties. Although we observed catalytic activity for the Cu(II)-$\mathbf{L^1}$ 1:1 system in the basic pH range, this effect is related to the trinuclear complexes which are also present in the solution. Therefore, further kinetic experiments were performed only at 3:2 ($\mathbf{L^1}$) and 2:1 ($\mathbf{L^2}$) copper(II)-to-ligand ratios.

The pH–$k_{obs,corr}$ profiles of catalytic H_2DTBC oxidation (Fig. S10) are distinctly different in the two systems. In case of Cu(II)-$\mathbf{L^1}$ complexes we observed a reproducible local

View Article Online
DOI: 10.1039/C6NJ03126A

maximum around pH 7.8 (Fig. S10) and increasing rate constants above pH 8.3. In presence of Cu(II)-$\mathbf{L^2}$ 2:1 complexes, a continuous increase of rate constants was observed above pH 7 (Fig. S10), and their values are higher at any pH than in the former case. The speciation of the complexes in 50% ethanol-water solvent mixture should only be slightly different from those determined in pure aqueous solutions, thus the observed catalytic activity is mainly related to the complexes $Cu_3H_{-1}\mathbf{L^1}_2$/$Cu_3H_{-3}\mathbf{L^1}_2$ and $Cu_2H_{-3}\mathbf{L^2}$ (Fig. S10). Based on these data (and to avoid the high rate of the autooxidation of H_2DTBC) the further kinetic measurements have been performed at pH = 7.8 ($\mathbf{L^1}$) and 8.9 ($\mathbf{L^2}$).

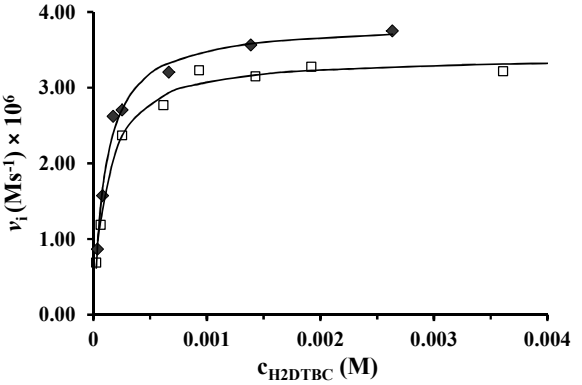

Figure 8 Dependence of the initial reaction rate on the H_2DTBC concentration promoted by Cu(II)-$\mathbf{L^1}$ 3:2 (♦, pH 7.8, $c_{complex} = 5.0\times10^{-5}$ M) and Cu(II)-$\mathbf{L^2}$ 2:1 (□, pH 8.9, $c_{complex} = 1\times10^{-5}$ M) systems (solid lines are fitted curves, see text).

The initial reaction rates of the catalytic oxidation as a function of H_2DTBC concentration (Fig. 8) show saturation kinetics above 10-50 fold excess of substrate over the complexes. This indicates a fast pre-equilibrium between the complex and the substrate molecules before the rate determining redox processes, therefore the Michaelis-Menten enzyme kinetic model is applicable in our systems. Table 3 lists the calculated Michaelis-Menten parameters of the two systems, along with those of some previously reported model complexes.

Table 3 Comparison of catecholase activity of some previously investigated copper(II)-ligand systems along with the catechol oxidase enzyme.

Cu(II)-ligand systems (*pH*)	k_{cat} (s^{-1})	K_M (M)	k_{cat}/K_M ($M^{-1}s^{-1}$)	Solvent, T (°C)	Ref.
Cu(II)-Ac-HHGH 1:1 (*10.18*)	0.063	not rep.	not rep.	MeOH/H_2O 86/14, 25	9
Cu(II)-MDVFMKGLSKAKEGV-NH_2 1:2 (*7.4*)	0.009	1.8×10^{-3}	5.0	MeOH/H_2O 80/20, 25	37
Cu(II)-B1[a] 2:1 (*8.50*)	0.051	9.44×10^{-3}	5.47	MeOH/H_2O 97/13, 25	91
Cu(II)-B2[a] 2:1 (*8.50*)	0.0078	9.5×10^{-4}	8.1	MeOH/H_2O 97/13, 25	91
Cu(II)-B3[b] 1:2	0.00596	2.6×10^{-4}	23.37	DMF, 20	76

View Article Online
DOI: 10.1039/C6NJ03126A

Cu(II)-B4[c] 2:1	0.25	6.4×10^{-3}	39.1	MeCN, 25	90
Cu(II)-B5[d] 2:4:2	0.0426	1.45×10^{-4}	293.8	MeOH, 25	89
Cu(II)-B6[e] 2:2	2.63	5.90×10^{-3}	445.8	MeOH, not rep.	88
Cu(II)-L[1] 3:2 (*7.8*)	**0.071**	**1.12×10^{-4}**	**632.1**	**EtOH/H_2O 50/50, 25**	
Cu(II)-B7[f] 2:1	1.916	1.2×10^{-3}	1597	MeCN, 25	87
Cu(II)-B8[g] 2:1 (8.0)	1.806	7.5×10^{-4}	2408	MeOH/H_2O 29/1, 20	71
Cu(II)-L[2] 2:1 (*8.9*)	**0.387**	**1.07×10^{-4}**	**3625**	**EtOH/H_2O 50/50, 25**	
Cu(II)-B9[h] 2:1	9	2.3×10^{-3}	3913	MeOH, 20	68
ibCO[i] (*6.5*)	2293	2.5×10^{-3}	917200	H_2O, 20	79

[a]ligand B1: *N',N'*-bis(2-pyridylmethyl)-*N,N*-(2-hydroxybenzyl)(2-hydroxy-3,5-di-*tert*-butylbenzyl)-1,3-propanediamin-2-ol; ligand B2: *N*-(2-hydroxybenzyl)-*N',N',N*-tris(2-pyridylmethyl)-1,3-propanediamin-2-ol
[b]ligand B3: 3-(3'-methyl-2'-pyridylimino)isoindoline-1-one (MePyOIND)
[c]ligand B4: 2,6-bis[bis(pyridin-2-ylmethylamino)methyl]-4-methylphenol (BPMP)
[d]ligand B5: naproxen (nap) and 3-picoline (3-pic)
[e]ligand B6: the copper(II) complex is referred as bis[1,2-*O*-isopropylidene-6-*N*-(3-acetylbut-3-en-2-one)amino-6-deoxyglucofuranoso]dicopper ($H_2$3a)
[f]ligand B7: $L^{1*}SSL^{1*}$
[g]ligand B8: a pyrazolate-derived compartmental ligand bearing pyridyl arms (HL^2)
[h]ligand B9: 2,6-bis(R-iminomethyl)-4-methyl-phenolato type Schiff-base ligand (H_2L2)
[i]native enzyme isolated from *Ipomoea batatas*; kinetic parameters reported for catechol substrate

Although the comparison with literature data is complicated by the many different conditions used, the presently studied copper(II) complexes possess high activities, outperforming the few copper(II)-peptide complexes reported earlier.[9,37] Regarding the non-peptide complexes, the k_{cat} values determined here can be considered average, however the k_{cat}/K_M ratios, especially in case of Cu(II)-**L[2]** 2:1, support the high efficiency of the present systems, due to the rather strong substrate binding (K_M). Nevertheless, these catalytic activities are more than 3 orders of magnitude lower than that of the native enzyme isolated from sweet potato.[79]

We also studied the performance of our complexes under real catalytic conditions, *i.e.* in presence of ~120 eq. excess of substrate ($c_{complex}$ = 1×10^{-5} M), following the reaction for longer time. After 1 hour, experimental turnover numbers of 41.1 h^{-1} (Cu(II)-**L[1]** 3:2, pH 7.8) and 64.1 h^{-1} (Cu(II)-**L[2]** 2:1, pH 8.9) was found, however these data are strongly affected by the diffusion rate of dioxygen into the studied solution.

In order to have more insights into the mechanism of H_2DTBC oxidation, reaction rates were measured as a function of complex and dioxygen concentration under pseudo-first order conditions. In all cases first order dependence was observed (Figs. S11, S12), which is in agreement with many other catecholase model systems.[69-72] According to the Michaelis-Menten model, the observed pseudo-second order reaction rate constant (*k'*, slope of the lines in Figure S11) is equal to $k_{cat}/(K_M + [S])$. The values calculated from the Michaelis-Menten

View Article Online
DOI: 10.1039/C6NJ03126A

parameters ($k'_{calc,\mathbf{L^1}}$ = 13.9 $M^{-1}s^{-1}$, $k'_{calc,\mathbf{L^2}}$ = 670.5 $M^{-1}s^{-1}$) are close to the measured ones ($k'_{\mathbf{L^1}}$ = 7.97 $M^{-1}s^{-1}$ and $k'_{\mathbf{L^2}}$ = 495.9 $M^{-1}s^{-1}$, Figure S11), which confirms the validity of our kinetic data.

3.6. Substrate binding study

4-Nitrocatechol binding. The three metal centers in $Cu_3H_x\mathbf{L^1}_2$ complexes may raise the question about the number of bound catechols in the fast pre-equilibrium step. Therefore, we studied the binding of 4-nitrocatechol ($H_2$4NC), a widely used chromophoric probe to mimic catechol-metal ion interaction.[80,81] Since this electron-poor catechol ligand possesses higher redox potential than H_2DTBC, its metal ion binding can be easily monitored by UV-Vis spectroscopy under aerobic conditions. First, the p*K* values and the spectral properties of $H_2$4NC have been determined in 50% EtOH/H_2O solvent (Table 4). The p*K* values of this ligand are considerably lower than those of H_2DTBC, thus the formation of ternary species with $Cu_3H_x\mathbf{L^1}_2$ complexes is expected at lower pH.

Table 4 UV-Vis spectroscopic parameters and deprotonation constants of 4-nitrocatechol ($H_2$4NC) substrate analogue (EtOH/H_2O 50/50, T = 298 K, I = 0.1 M NaCl). Calculated individual molar spectra in Fig. 9 insert.

	λ_{max} (nm)	$\varepsilon_{\lambda_{max}}$ ($M^{-1}cm^{-1}$)	p*K*
$H_2$4NC	350	7925	6.78(2)
$[H4NC]^-$	434	15545	11.78(1)
$[4NC]^{2-}$	512	13446	

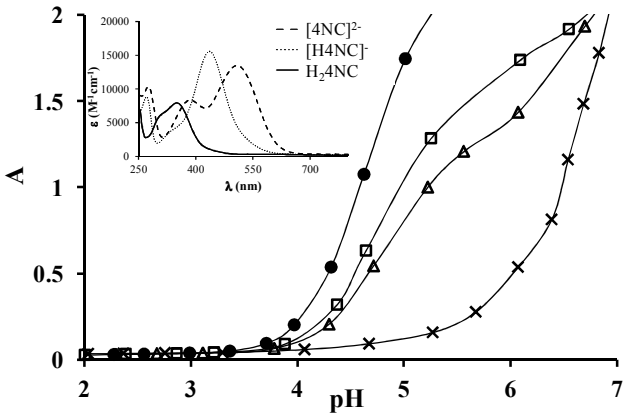

Figure 9 pH-dependent absorption at 434 nm at different Cu(II)-$\mathbf{L^1}$-$H_2$4NC ratios: × 0:0:1, ● 3:2:1, □ 3:2:2, Δ 3:2:3 (c_{H_24NC} = 2.5×10^{-4} M, in EtOH/H_2O 50/50). Insert: Individual molar spectra of differently protonated 4NC species.

View Article Online
DOI: 10.1039/C6NJ03126A

pH-dependent absorption spectra of Cu(II)-$\mathbf{L^1}$-$H_2$4NC ternary systems were followed at different complex-to-$H_2$4NC ratios (Fig. 9 and Fig. S13). Fig. 9 shows the change of absorbance at 434 nm in function of pH. At 1:1 complex-to-$H_2$4NC ratio, the pK of $H_2$4NC deprotonation is considerably shifted to the acidic region (from pK = 6.78 to ~4.5), clearly indicating direct binding of catechol to the complexes resulting in metal-induced deprotonation. With decreasing concentration of the trinuclear complexes the deprotonation of $H_2$4NC follows a two-step process indicating that only one equivalent catecholate is coordinated under our conditions (the excess $H_2$4NC deprotonates at higher pH, without the participation of the copper(II) complexes). Since the coordination of the analogous monodentate 4-nitrophenol was not observed in a similar experiment, bidentate coordination of the catechol substrates can be suggested.

H_2DTBC binding (anaerobic conditions). Figs. 10 and S14 show the UV-Vis spectra of Cu(II)-$\mathbf{L^1}$-H_2DTBC ternary system at pH 7.8 with increasing H_2DTBC concentrations.

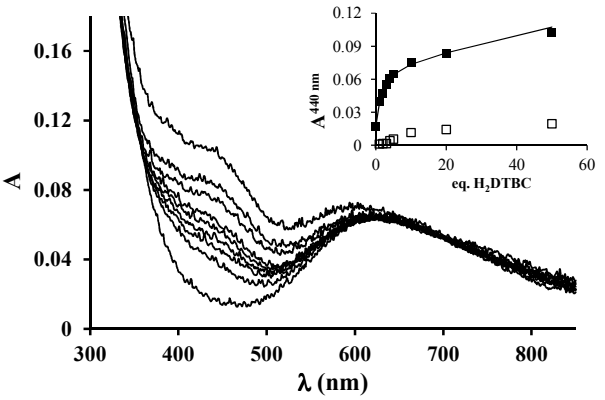

Figure 10 H_2DTBC-dependent UV-Vis spectra of Cu(II)-$\mathbf{L^1}$ 3:2 system under anaerobic conditions ($c_{complex}$ = 2.4×10^{-4} M, in EtOH/H_2O 50/50, pH 7.8). Insert: Absorbance at 440 nm in function of eq. H_2DTBC in presence (■) and in absence (□) of Cu(II)-$\mathbf{L^1}$ 3:2 system (solid line is fitted curve, see text).

Three new bands appear on the electronic absorption spectra at 280, 300 and 440 nm. The wide band at 440 nm and the shoulder around 300 nm (Fig. S14) are related to the ternary species $Cu_3H_x\mathbf{L^1}_2(DTBC^{2-})$ in agreement with earlier reports on the spectral behavior of Cu^{2+}-ligand-catecholate ternary complexes,[68,70] while the band at 280 nm belongs to the absorption of H_2DTBC itself. The d-d absorption band of Cu(II) around 625 nm is almost unchanged during the experiment, only a slight blue shift indicates the alteration of the coordination sphere around the metal ion. In addition, the characteristic absorption band of the oxidized

View Article Online
DOI: 10.1039/C6NJ03126A

3,5-di-*tert*-butyl benzoquinone (DTBQ) product does not appear around 400 nm. These facts indicate that under anaerobic conditions the formation of the copper(II)-catecholate ternary species is not followed by the reduction of Cu^{2+} ions (and the oxidation of the substrate).

The insert in Fig. 10 depicts the change of absorbance at 440 nm indicating nearly complete formation of the ternary species at ten-fold excess of the substrate. From the non-linear regression of these data K_{app} = 3570 M^{-1} can be calculated (see the solid line of the insert) for the apparent formation constant of the reaction $Cu_3H_x\mathbf{L^1}_2$ + H_2DTBC = $Cu_3H_y\mathbf{L^1}_2$(DTBC^{2-}). In fact, this reaction is the pre-equilibrium according to the Michealis-Menten formalism. The value $1/K_{app}$ = 0.28 mM is in good agreement with K_M = 0.12 mM obtained from the kinetic data, which confirms the high binding ability of H_2DTBC to the trinuclear complexes.

Based on these results, the role of dioxygen is the oxidation of the substrate activated by the copper(II)-$\mathbf{L^1}$ complexes, and not the regeneration of the Cu^{2+} complex (re-oxidation of Cu^{+}), as it was proposed for the native enzyme,[66,67] and for many catalytic dinuclear copper(II) complexes.[82] In fact, the observed phenomenon is in agreement with an oxidation pathway used by mononuclear copper(II) complexes,[70,75] involving the formation of radical intermediate(s) (see later).

Anaerobic UV-Vis measurements on the H_2DTBC binding were carried out in the Cu(II)-$\mathbf{L^2}$ 2:1 system, too. Fig. 11 shows the recorded spectra in presence of 0 to 3 eq. H_2DTBC.

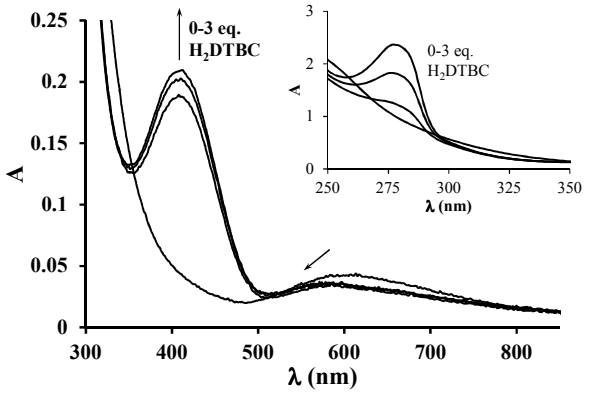

Figure 11 H_2DTBC-dependent UV-Vis spectra of Cu(II)-$\mathbf{L^2}$ 2:1 system under anaerobic conditions ($c_{complex}$ = 2.4×10^{-4} M, in EtOH/H_2O 50/50, pH 8.9). Insert: UV region of the measured spectra.

The observations are fundamentally different from the previous system: the strong absorbance of DTBQ at 400 nm appeared immediately after the introduction of 1 eq. substrate in absence of dioxygen and the intensity of the Cu(II) d-d band decreased. Further additions

View Article Online
DOI: 10.1039/C6NJ03126A

of H_2DTBC result the formation of some additional DTBQ. Though the decrease of Cu(II) band intensity is undeniable, the entire disappearance of the signal does not occur, *i.e.* the redox reaction is not stoechiometric. This is consistent with many previous observations that the reduction of copper(II) under anaerobic conditions is not complete until the introduction of considerable excess of H_2DTBC.[72,78] These results indicate a single-step two-electron oxidation of the catechol substrate by the two cooperating copper(II) centers in the Cu(II)-$\mathbf{L^2}$ complexes, which is the main proposed mechanism for binuclear catecholase-like copper(II) complexes.[82]

3.7 Peroxide, o-benzoquinone and radical formation during the oxidation of H_2DTBC

The detection and quantification of H_2O_2 has been accomplished by treating the aqueous phase with acidic $TiOSO_4$ solution, after elimination the remaining H_2DTBC and DTBQ by dichloromethane extraction. The concentration of peroxotitanyl complex was measured spectrophotometrically at 408 nm (see also the experimental part). The formation of DTBQ and H_2O_2 has been determined parallel during the copper(II) catalyzed reaction of H_2DTBC. Both catalytic systems show initial accumulation of H_2O_2 in the beginning of the reaction, followed by its slow decay (Fig. S15). Moreover, the concentration of the formed DTBQ exceeds considerably the peroxide level in both cases. This suggests a dynamic equilibrium of H_2O_2 between its formation and consumption after the initial stages of the catalytic reaction.

As described above, under anaerobic conditions the formation of copper(II)-catecholate unit was observed in the Cu(II)-$\mathbf{L^1}$-H_2DTBC system (Fig. 10), without the subsequent redox reaction between Cu(II) and the substrate. This is consistent with mononuclear catalytic centers, where valence tautomer (VT) equilibrium between the copper(II)-catecholate and copper(I)-semiquinone adduct is strongly dependent on the donor groups and structure of the applied ligand.[82,83] Both tautomer forms are oxygen sensitive, therefore the catalytic oxidation should proceed through the formation of radial intermediates (semiquinone (SQ), superoxide radical or both). Radicals can be detected by EPR. Although copper(II)-superoxide complexes are generally EPR silent due to the antiferromagnetic interaction,[85,86] the formation of SQ intermediates has been previously observed by EPR.[69,75-77] Therefore, we attempted to detect the formation of radical intermediate(s) in both aerobic and anaerobic conditions. In the absence of dioxygen radicals were not detected, according to the anaerobic UV-Vis measurement of the Cu(II)-$\mathbf{L^1}$-H_2DTBC system. Under aerobic conditions, however, a well-defined doublet EPR signal ($g = 2.0046 \pm 0.0001$, $a_H = 2.67$ G, Fig. 12) was observed, similarly to those detected earlier for intermediates of H_2DTBC oxidation.[75-77] Hence, we must

View Article Online
DOI: 10.1039/C6NJ03126A

conclude that in the copper(II)-$\mathbf{L^1}$-H_2DTBC system the copper(II)-bound catecholate is oxidized only in the presence of dioxygen, through the formation of oxygenated radical intermediate (Scheme 2).

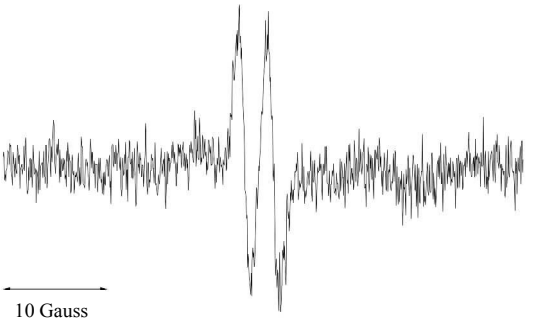

Figure 12 EPR spectrum of the radical formed under aerobic reaction conditions in the Cu(II)-$\mathbf{L^1}$-H_2DTBC system (in EtOH/H_2O 50/50, $c_{complex} = 5\times10^{-5}$ M, $c_{H_2DTBC} = 2\times10^{-3}$ M, pH = 8).

3.8. Mechanism of catecholase activities of copper(II)-L^1 and -L^2 systems

Based on the detailed kinetic study and careful evaluation of the substrate binding experiments, the oxidation of H_2DTBC catalyzed by the oligonuclear copper(II) complexes of $\mathbf{L^1}$ and $\mathbf{L^2}$ proceeds via the one- and two-electron transfer from catechol to the copper(II) ion(s), respectively. Scheme 4 presents the suggested basic reaction steps of the catalytic oxidation of H_2DTBC.

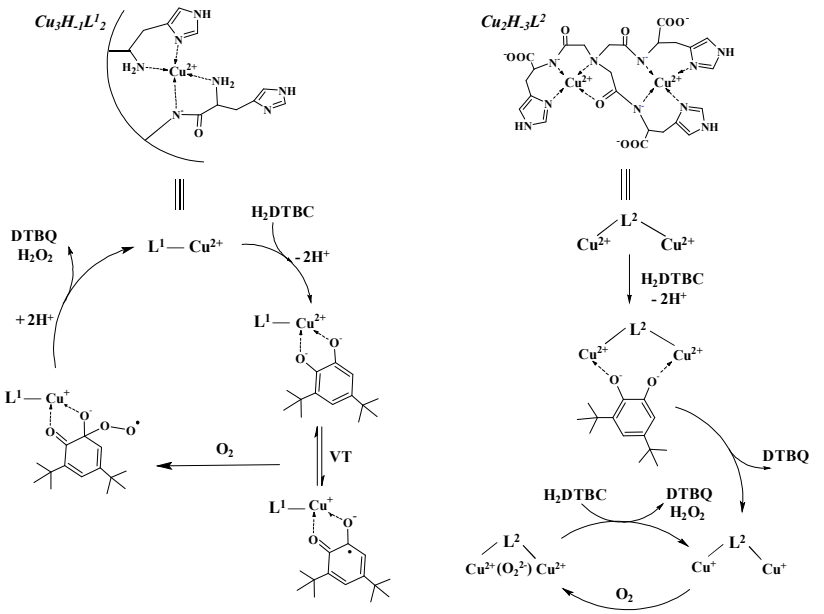

Scheme 4 Proposed mechanism of catalytic oxidation of 3,5-di-*tert*-butylcatechol by $\mathbf{L^1}$ and $\mathbf{L^2}$ ligand-copper(II) systems.

View Article Online
DOI: 10.1039/C6NJ03126A

Under the conditions used for $\mathbf{L^1}$ (pH 7.8, Cu(II)/$\mathbf{L^1}$ = 3/2) trinuclear complexes (mostly $Cu_3H_{-1}\mathbf{L^1}_2$) are the pre-active species. Nevertheless, oxidation of H_2DTBC proceeds in a one-electron transfer pathway, with the participation of a single Cu^{2+} center; the other metal ions might only have inferior contribution in substrate binding. In this system the copper(II)-catecholate/copper(I)-semiquinone valence tautomerism (VT) is shifted towards the copper(II)-catecholate form. One of these tautomers reacts with dioxygen in the rate determining step, resulting the formation of oxygenated radical intermediate(s). After a subsequent intramolecular electron transfer DTBQ and H_2O_2 molecules are released, regenerating the copper(II) center and allowing the coordination of a new substrate.

In contrast, the oxidation in the Cu(II)-$\mathbf{L^2}$-H_2DTBC system is catalyzed by two co-operating copper(II) centers, similarly to the catecholase enzymes. Even though dicopper(II) species are formed already at pH 4 in Cu(II)-$\mathbf{L^2}$ 2:1 system, the tendency of catecholase-like activity follows the formation of $Cu_2H_{-3}\mathbf{L^2}$. After coordination of the substrate to the dicopper(II) core, DTBQ and dicopper(I) species are formed in a fast electron transfer process. The reduced metal centers are re-oxidized by dioxygen, yielding probably a Cu(II)-O_2^{2-}-Cu(II) species, as it is often proposed.[82] This in turn reacts with an incoming second substrate molecule, and the dicopper(I) species is regenerated after releasing the second DTBQ and H_2O_2 (via proton transfer).

Since hydrogen peroxide does not seem to be produced in stoichiometric quantity in either catalytic system, the participation of H_2O_2 in the catalytic reaction can be suggested. Most probably, as a widely known oxidizing agent, the peroxide molecule might contribute to the reoxidation of Cu(I) center(s) to Cu(II), as it was previously described for other catalytic copper(II) complexes.[73,74]

It is interesting to note, that in case of both ligands amide coordinated complexes are the pre-active species during H_2DTBC oxidation. Although the reactivity of catecholates increases considerably with increasing pH, the thermodynamic stability of amide coordinated complexes also increases, thus the +2 oxidation state of copper becomes more stabilized. Therefore, we hypothesize that the deprotonated amides may facilitate the coordination of catechols by abstracting protons (re-protonation), which opens the possibility for the formation of copper(I) complexes.

View Article Online
DOI: 10.1039/C6NJ03126A

4. Conclusions

Taking advantage of the preorganized structure of tripodal scaffolds and the metal binding ability of histidine units, we intend to develop new peptide ligands able to form oligonuclear copper(II) core. For this purpose synthesized two histidine derivatives based on tren and nta as tripodal platforms, which contain three non-protected N-terminal ($\mathbf{L^1}$) and C-terminal ($\mathbf{L^2}$) histidines. At 1:1 metal-to-ligand ratio and above pH 9 the participation of the tertiary amine in the fused chelate rings results in unique binding mode in both $CuH_{-2}\mathbf{L^1}$ and $CuH_{-2}\mathbf{L^2}$. On the other hand, between pH 4-9 the two ligands behave as the corresponding dipeptides containing N/C-terminal histidines, which results in one ($\mathbf{L^1}$) or two ($\mathbf{L^2}$) 'legs' available for further metal ion binding. As a consequence, oligonuclear complexes are formed at metal ion excess with 3/2 ($\mathbf{L^1}$) and 2/1 ($\mathbf{L^2}$) metal-to-ligand ratios. Above pH 7, the oligonuclear complexes of both ligands have considerable catecholase-like activity, although the two systems operate with distinctly different mechanisms. The oxidation of H_2DTBC proceeds in a one-electron transfer pathway, with the participation of a single Cu^{2+} center in presence of $\mathbf{L^1}$ complexes. On the other hand, the proximity of the two metal ions in the dinuclear complexes of $\mathbf{L^2}$ allows their cooperation along the catalytic cycle, resulting efficient catalytic oxidation of 3,5-di-*tert*-butyl-catechol.

Acknowledgement. This work was supported by the Hungarian Scientific Research Fund (OTKA K101541). The authors warmly thank A. Merlin and S. Parant for technical help, and F. Lachaud for MS measurements at Université de Lorraine.

Appendix A. Supplementary material

Supplementary data associated with this article can be found in the online version, at doi:????.

View Article Online
DOI: 10.1039/C6NJ03126A

References

[1] T. Gajda, B. Henry, A. Aubry and J.-J. Delpuech, *Inorg. Chem.*, 1996, **35**, 586–593.
[2] C. Harford and B. Sarkar, *Acc. Chem. Res.*, 1997, **30**, 123–130.
[3] D. Valensin, M. Luczkowski, F. M. Mancini, A. Legowska, E. Gaggelli, G. Valensin, K. Rolka and H. Kozlowski, *Dalton Trans.*, 2004, **9**, 1284–1293.
[4] D. Valensin, F. M. Mancini, M. Luczkowski, A. Janicka, K. Wisniewska, E. Gaggelli, G. Valensin, L. Lankiewicz and H. Kozlowski, *J. Chem. Soc. Dalton Trans.*, 2004, **1**, 16–22.
[5] K. Ősz, Z. Nagy, G. Pappalardo, G. Di Natale, D. Sanna, G. Micera, E. Rizzarelli and I. Sóvágó, *Chem. Eur. J.*, 2007, **13**, 7129–7143.
[6] A. Kolozsi, A. Jancsó, N. V. Nagy and T. Gajda, *J. Inorg. Biochem.*, 2009, **103**, 940–947.
[7] G. Di Natale, K. Ősz, Cs. Kállay, G. Pappalardo, D. Sanna, G. Impellizzeri, I. Sóvágó and E. Rizzarelli, *Chem. Eur. J.*, 2013, **19**, 3751–3761.
[8] D. Árus, N. V. Nagy, Á. Dancs, A. Jancsó, R. Berkecz and T. Gajda, *J. Inorg. Biochem.*, 2013, **126**, 61–69.
[9] A. Jancsó, Z. Paksi, N. Jakab, B. Gyurcsik, A. Rockenbauer and T. Gajda, *Dalton Trans.*, 2005, **19**, 3187–3194.
[10] Z. Paksi, A. Jancsó, F. Pacello, N. V. Nagy, A. Battistoni and T. Gajda, *J. Inorg. Biochem.*, 2008, **102**, 1700–1710.
[11] D. Árus, A. Jancsó, D. Szunyogh, F. Matyuska, N. V. Nagy, E. Hoffmann, T. Körtvélyesi and T. Gajda, *J. Inorg. Biochem.*, 2012, **106**, 10–18.
[12] S. Timári, R. Cerea and K. Várnagy, *J. Inorg. Biochem.*, 2011, **109**, 1009–1017.
[13] Y. Jin and J. A. Cowan, *J. Am. Chem. Soc.*, 2005, **127**, 8408–8415.
[14] E. Kopera, A. Krężel, A. M. Protas, A. Belczyk, A. Bonna, A. Wysłouch-Cieszyńska, J. Poznański and W. Bal, *Inorg. Chem.*, 2010, **49**, 6636−6645.
[15] A. Fragoso, P. Lamosa, R. Delgado and O. Iranzo, *Chem. Eur. J.*, 2013, **19**, 2076–88.
[16] H. B. Albada and R. M. J. Liskamp, *J. Comb. Chem.*, 2008, **10**, 814–824.
[17] A. M. Pujol, C. Gateau, C. Lebrun and P. Delangle, *J. Am. Chem. Soc.*, 2009, **131**, 6928–6929.
[18] A. Pujol, C. Gateau, C. Lebrun and P. Delangle, *Chem. Eur. J.*, 2011, **17**, 4418–4428.
[19] A.-S. Jullien, C. Gateau, I. Kieffer, D. Testemale and P. Delangle, *Inorg. Chem.*, 2013, **52**, 9954–9961.
[20] A.-S. Jullien, C. Gateau, C. Lebrun and P. Delangle, *Inorg. Chem.*, 2015, **54**, 2339–2344.
[21] M. Gelinsky, R. Vogler and H. Vahrenkamp, *Inorg. Chem.*, 2002, **41**, 2560–2564.
[22] U. Herr, W. Spahl, G. Trojandt, W. Steglich, F. Thaler and R. van Eldik, *Bioorg. Biomed. Chem.*, 1999, **7**, 699–707.
[23] M. M. Ibrahim, N. Shimomura, K. Ichikawa and M. Shiro, *Inorg. Chim. Acta*, 2001, **313**, 125–136.
[24] M. M. Ibrahim and G. A. M. Mersal, *J. Inorg. Biochem.*, 2010, **104**, 1195–1204.
[25] H. B. Albada, F. Soulimani, B. M. Weckhuysen and R. M. J. Liskamp, *Chem. Commun.*, 2007, **46**, 4895–4897.
[26] A. Messadi, A. Mohamadou, I. Déchamp-Olivier and L. Dupont, *J. Coord. Chem.*, 2012, **65**, 2442–2458.
[27] Ł. Szyrwiel, Ł. Szczukowski, J. S. Pap, B. Setner, Z. Szewczuk and W. Malinka, *Inorg. Chem.*, 2014, **53**, 7951–7959.
[28] Ł. Szyrwiel, J. S. Pap, Ł. Szczukowski, Zs. Kerner, J. Brasun, B. Setner, Z. Szewczuk and W. Malinka, *RSC Adv.*, 2015, **5**, 56922–56931.
[29] D. F. Shullenberger, P. D. Eason and E. C. Long, *J. Am. Chem. Soc.*, 1993, **115**, 11038-11039.
[30] I. V. J. Murray, M. E. Sindoni and P. H. Axelsen, *Biochemistry*, 2005, **44**, 12606–12613.

View Article Online
DOI: 10.1039/C6NJ03126A

[31] F. Haeffner, D. G. Smith, K. J. Barnham and A. I. Bush, *J. Inorg. Biochem.*, 2005, **99**, 2403–2422.
[32] G. F. Z. da Silva, W. M. Tay and Li-June Ming, *J. Biol. Chem.*, 2005, **17**, 16601–16609.
[33] G. F. Z. da Silva and L.-J. Ming, *Angew. Chem., Int. Ed.*, 2005, **44**, 5501–5504.
[34] G. F. Z. da Silva and L.-J. Ming, *Angew. Chem., Int. Ed.*, 2007, **46**, 3337–3341.
[35] D. Ciregna, E. Monzani, G.Thiabaud, S. Pizzocaro and L. Casella, *Chem. Commun.,* 2013, **49**, 4027–4029.
[36] W. M. Tay, Ahmed I. Hanafy, A. Angerhofer and L.-J. Ming, *Bioorg. Med. Chem. Lett.*, 2009, **19**, 6709–6712.
[37] S. Dell'Acqua, V. Pirota, C. Anzani, M. M. Rocco, S. Nicolis, D. Valensin, E. Monzania and L. Casella, *Metallomics*, 2015, **7**, 1091–1102.
[38] F. J. C. Rosotti and H. Rosotti, *The determination of stability constants*, McGraw-Hill Book Co., New York, 1962, p. 149.
[39] E. Högfeldt, *Stability Constants of Metal-Ion Complexes, Part A. Inorganic Ligands*, Pergamon, New York, 1982, p. 32.
[40] L. Zékány, I. Nagypál and G. Peintler, *PSEQUAD for chemical equilibria*, Technical Software Distributors: Baltimore, MD, 1991.
[41] A. Rockenbauer, T. Szabó-Plánka, Zs. Árkosi and L. Korecz, *J. Am. Chem. Soc.*, 2001, **123**, 7646–7654.
[42] A. Rockenbauer and L. Korecz, *Appl. Magn. Reson*., 1996, **10**, 29–43.
[43] R. G. Bates, M. Paabo and R. A. Robinson, *J. Phys. Chem*., 1963, **67**, 1833–1838.
[44] E. M. Woolley, D. G. Hurkot and L. G. Hepler, *J. Phys. Chem*., 1970, **74**, 3908–3913.
[45] D. R. Lide, *CRC Handbook of Chemistry and Physics*, Taylor and Francis, 88th Ed. 2007-2008., p. 8–81.
[46] A. G. Blackman, *Polyhedron*, 2005, **24**, 1–39.
[47] Cs. Kállay, K. Várnagy, G. Malandrinos, N. Hadjiliadis, D. Sanna and I. Sóvágó, *Inorg. Chim. Acta*, 2009, **362**, 935–945.
[48] I. Sóvágó, *Biocoordination Chemistry, ch.: Metal complexes of peptides and their derivatives*, ed. K. Burger, Ellis Horwood, Chichester, 1990.
[49] I. Sóvágó and K. Ősz, *Dalton Trans.*, 2006, **32**, 3841–3854.
[50] S. Sjöberg, *Pure Appl. Chem.*, 1997, **69**, 1549–1570.
[51] I. Török, T. Gajda, B. Gyurcsik, G. K. Tóth and A. Péter, *J. Chem. Soc., Dalton Trans.*, 1998, 1205–1212.
[52] A. Ensuque, A. Demaret, L. Abello and G. Lapluye, *J. Chim. Phys.*, 1982, **79**, 185–188.
[53] B. Gyurcsik, I. Vosekalna and E. Larsen, *J. Inorg. Biochem.*, 2001, **85**, 89–98.
[54] N. I. Jakab, B. Gyurcsik, T. Körtvélyesi, I. Vosekalna, J. Jensen and E. Larsen, *J. Inorg. Biochem.*, 2007, **101**, 1376–1385.
[55] A. P. Garnett and J. H. Viles, *J. Biol. Chem.*, 2003, **278**, 6795–6802.
[56] E. Aronoff-Spencer, C. S. Burns, N. I. Avdievich, G. J. Gerfen, J. Peisach, W. E. Antholine, H. L. Ball, F. E. Cohen, S. B. Prusiner and G. L. Millhauser, *Biochemistry*, 2000, **39**, 13760–13771.
[57] P. Lubal, M. Kývala, P. Hermann, J. Holubová, J. Rohovec, J. Havel and I. Lukes, *Polyhedron*, 2001, **20**, 47–55.
[58] G. Greiner, L. Seyfarth, W. Poppitz, R. Witter, U. Sternberg and S. Reissmann, *Lett. Pept. Sci.*, 2000, **7**, 133–141.
[59] K. Ősz, K. Várnagy, H. Süli-Vargha, D. Sanna, G. Micera and I. Sóvágó, *J. Chem. Soc. Dalton Trans.*, 2003, **10**, 2009–2016.
[60] I. Sóvágó, E. Farkas and A. Gergely, *J. Chem. Soc. Dalton Trans.*, 1982, 2159–2163.
[61] S. Bruni, F. Cariati, P. G. Daniele and E. Prenesti, *Spectrochim. Acta A*, 2000, **56**, 815–827.

View Article Online
DOI: 10.1039/C6NJ03126A

[62] T. Gajda, B. Henry and J. Delpuech, *J. Chem. Soc. Dalton Trans.*, 1993, 1303–1310.
[63] D.-H. Lee, N. N. Murthy and K. D. Karlin, *Inorg. Chem.*, 1997, **36**, 5785–5792.
[64] B. Bóka, A. Myari, I. Sóvágó and N. Hadjiliadis, *J. Inorg. Biochem.*, 2004, **98**, 113–122.
[65] E. Prenesti, P. G. Daniele, M. Prencipe and G. Ostacoli, *Polyhedron*, 1999, **18**, 3233–3241.
[66] T. Klabunde, C. Eicken, J. C. Sachettini and B. Krebs, *Nat. Struct. Biol*., 1998, **5**, 1084–1090.
[67] N. Hakulinen, C. Gasparetti, H. Kaljunen, K. Kruus and J. Rouvinen, *J. Biol. Inorg. Chem.*, 2013, **18**, 917.
[68] K. S. Banu, T. Chattopadhyay, A. Banerjee, S. Bhattacharya, E. Suresh, M. Nethaji, E. Zangrando and D. Das, *Inorg. Chem.*, 2008, **47**, 7083–7093.
[69] I. A. Koval, K. Selmeczi, C. Belle, C. Philouze, E. Saint-Aman, I. Gautier-Luneau, A. M. Schuitema, M. van Vliet, P. Gamez, O. Roubeau, M. Lueken, B. Krebs, M. Lutz, A. L. Spek, J.-L. Pierre and J. Reedijk, *Chem. Eur. J.*, 2006, **12**, 6138–6150.
[70] M. Kodera, T. Kawata, K. Kano, Y. Tachi, S. Itoh and S. Kojo, *Bull. Chem. Soc. Jpn.*, 2003, **76**, 1957–1964.
[71] J. Ackermann, S. Buchler and F. Meyer, *C. R. Chimie*, 2007, **10**, 421–432.
[72] A. Granata, E. Monzani and L. Casella, *J. Biol. Inorg. Chem.*, 2004, **9**, 903–913.
[73] A. Neves, L. M. Rossi, A. J. Bortoluzzi, B. Szpoganicz, C. Wiezbicki, E. Schwingel, W. Haase and S. Ostrovsky, *Inorg. Chem.*, 2002, **41**, 1788–1794.
[74] E. Monzani, L. Quinti, A. Perotti, L. Casella, M. Gullotti, L. Randaccio, S. Geremia, G. Nardin, P. Faleschini and G. Tabbi, *Inorg. Chem.*, 1998, **37**, 553–562.
[75] J. Kaizer, J. Pap, G. Speier, L. Párkányi, L. Korecz and A. Rockenbauer, *J. Inorg. Biochem.,* 2002, **91**, 190–198.
[76] J. Kaizer, T. Csay, G. Speier and M. Giorgi, *J. Mol. Catal. A: Chem.*, 2010, **329**, 71–76.
[77] T. Csay, B. Kripli, M. Giorgi, J. Kaizer and G. Speier, *Inorg. Chem. Comm.*, 2010, **13**, 227–230.
[78] E. Monzani, L. Casella, G. Zoppellaro, M. Gullotti, R. Pagliarin, R. P. Bonomo, G. Tabbi, G. Nardin and L. Randaccio, *Inorg. Chim. Acta*, 1998, **282**, 180-192.
[79] C. Eicken, F. Zippel, K. Buldt-Karentzopoulos and B. Krebs, *FEBS Lett.*, 1998, 436, 293–299.
[80] C. A. Tyson, *J. Biol. Chem*., 1975, **250**, 1765–1770.
[81] J. Kaizer, Z. Zsigmond, I. Ganszky, G. Speier, M. Giorgi and M. Réglier, *Inorg. Chem*., 2007, **46**, 4660–4666.
[82] I. A. Koval, P. Gamez, C. Belle, K. Selmeczi and J. Reedijk, *Chem. Soc. Rev.*, 2006, **35**, 814–840.
[83] G. Speier, Z. Tyeklár, P. Tóth, E. Speier, S. Tisza, A. Rockenbauer, A. M. Whalen, N. Alkire, and C. G. Pierpont, *Inorg. Chem.*, 2001, **40**, 5653–5659.
[84] K. J. Reszka and C. F. Chignell, *J. Am. Chem. Soc.*, 1993, **115**, 7152–1160.
[85] M. P. Lanci, V. V. Smirnov, C. J. Cramer, E. V. Gauchenova, J. Sundermeyer, J. P. Roth, *J. Am. Chem. Soc.*, 2007, **129**, 14697–14709.
[86] P. J. Donoghue, A. K. Gupta, D. W. Boyce, C. J. Cramer, and W. B. Tolman, *J. Am. Chem. Soc.*, 2010, **132**, 15869–15871.
[87] E. C. M. Ording-Wenker, M. A. Siegler, M. Lutz and E. Bouwman, *Dalton Trans.*, 2015, **44**, 12196–12209.
[88] R. Wegner, M. Gottschaldt, H. Gorls, E.-G. Jager and D. Klemm, *Chem. Eur. J.*, 2001, **7**, 2143–2157.
[89] S. Caglar, E. Adiguzel, B. Sariboga, E. Temel and O. Buyukgungor, *J. Coord. Chem.*, 2014, **67**, 670–683.

View Article Online
DOI: 10.1039/C6NJ03126A

[90] S. J. Smith, C. J. Noble, R. C. Palmer, G. R. Hanson, G. Schenk, L. R. Gahan and M. J. Riley, *J. Biol. Inorg. Chem.*, 2008, **13**, 499–510.
[91] R. E. H. M. B. Osorio, R. A. Peralta, A. J. Bortoluzzi, V. R. de Almeida, B. Szpoganicz, F. L. Fischer, H. Terenzi, A. S. Mangrich, K. M. Mantovani, D. E. C. Ferreira, W. R. Rocha, W. Haase, Z. Tomkowicz, A. dos Anjos and A. Neves, *Inorg. Chem.*, 2012, **51**, 1569–1589.

View Article Online
DOI: 10.1039/C6NJ03126A

Histidine-rich tripodal peptides form unique oligonuclear complexes with copper(II), which possess efficient catecholase-like activity.